Chemoenzymatic Synthesis, Characterization, and Scale-up of Milk Thistle Flavonolignan Glucuronides

Brandon T. Gufford, Tyler N. Graf, Noemi D. Paguigan, Nicholas H. Oberlies, and Mary F. Paine

Experimental and Systems Pharmacology (B.T.G, M.F.P), College of Pharmacy, Washington State University, Spokane, Washington; and Department of Chemistry and Biochemistry, The University of North Carolina at Greensboro, Greensboro, North Carolina (T.N.G, N.D.P., N.H.O)

Running Title: Synthesis and Characterization of Milk Thistle Glucuronides

Corresponding Author: Mary F. Paine, RPh, PhD

Experimental and Systems Pharmacology

WSU College of Pharmacy

PBS 323, PO Box 1495

Spokane, WA 99210-1495

Phone: 509-358-7759

Fax: 509-368-6561

Email: mary.paine@wsu.edu

Number of text pages: 15

Number of tables: 3

Number of figures: 8

Number of references: 46

Word Count

Total: 4,181

Abstract: 239

Introduction: 723

Discussion: 939

Abbreviations: BLM, bovine liver microsome; BSA, bovine serum albumin; COSY, correlation spectroscopy; HLM, human liver microsome; HSQC, heteronuclear single quantum correlation; HMBC, heteronuclear multiple bond correlation; HRESIMS, high resolution electrospray ionization mass spectrometry; m/z, mass-to-charge ratio; UDPGA, UDP-glucuronic acid; UGT, UDP-glucuronosyl transferase; UPLC, ultra-performance liquid chromatography

DMD Fast Forward. Published on August 27, 2015 as DOI: 10.1124/dmd.115.066076
This article has not been copyedited and formatted. The final version may differ from this version.

Abstract

Plant-based therapeutics, including herbal products, continue to represent a growing facet of the contemporary healthcare market. Mechanistic descriptions of the pharmacokinetics and pharmacodynamics of constituents composing these products remain nascent, particularly for metabolites produced following herbal product ingestion. Generation and characterization of authentic metabolite standards are essential to improve the quantitative mechanistic understanding of herbal product disposition in both in vitro and in vivo systems. Using the model herbal product, milk thistle, the objective of this work was to biosynthesize multi-mg quantities of glucuronides of select constituents (flavonolignans) to fill multiple knowledge gaps in the understanding of herbal product disposition and action. A partnership between clinical pharmacology and natural products chemistry expertise was leveraged to optimize reaction conditions for efficient glucuronide formation and evaluate alternate enzyme and reagent sources to improve cost-effectiveness. Optimized reaction conditions used at least one-fourth the amount of microsomal protein (from bovine liver) and cofactor (UDPGA) compared to typical conditions using human-derived subcellular fractions, providing substantial cost savings. Glucuronidation was flavonolignan-dependent. Silybin A, silybin B, isosilybin A, and isosilybin B generated five, four, four, and three mono-glucuronides, respectively. Large scale synthesis (40 mg starting material) generated three glucuronides of silybin A: silybin A-7-*O*-β-D-glucuronide (15.7 mg), silybin A-5-*O*-β-D-glucuronide (1.6 mg), and silybin A-4´´-*O*-β-D-glucuronide (11.1 mg). This optimized, cost-efficient method lays the foundation for a systematic approach to synthesize and characterize herbal product constituent glucuronides, enabling an improved understanding of mechanisms underlying herbal product disposition and action.

Introduction

Plant-based therapeutics, including herbal products, have existed for thousands of years, predating recorded history. Today, herbal products represent an ever-flourishing facet of the contemporary healthcare market, which has grown steadily in the United States since passage of the Dietary Supplement Health and Education Act in 1994 (Lindstrom et al., 2014). Despite millennia of usage, mechanistic descriptions of the pharmacokinetics and pharmacodynamics of constituents composing these products remain nascent.

The top-selling herbal product, milk thistle [*Silybum marianum* (L.) Gaertn. (Asteraceae)], is an extensively studied hepatoprotectant, as well as perpetrator of herb-drug interactions (Wellington and Jarvis, 2001; Gurley et al., 2006; Abenavoli et al., 2010; Brantley et al., 2010; Loguercio and Festi, 2011; Gurley, 2012; Gurley et al., 2012; Brantley et al., 2013; Polyak et al., 2013a; Polyak et al., 2013b; Brantley et al., 2014a; Brantley et al., 2014b; Gufford et al., 2014a; Gufford et al., 2015). Despite considerable investigation, quantitative data describing mechanisms underlying the disposition of milk thistle constituents remain elusive and are virtually nonexistent when considering herbal constituent metabolites generated in vivo. Failing to account for the disposition and possible bioactivity of these metabolites may be a source of frequently cited in vitro-in vivo disconnects when translating pre-clinical “hits” to clinical application (Won et al., 2010; Won et al., 2012). Generation and characterization of authentic metabolite standards of these constituents are essential to improve the quantitative mechanistic understanding of their disposition in both in vitro and in vivo systems.

Synthesis of metabolite standards of herbal products poses challenges beyond those with drug metabolites (Walker et al., 2011; Walker et al., 2014; Di and Obach, 2015). For example, because herbal products are plant-derived, product variation can occur at multiple stages of production, ranging from plant growth and sourcing to harvest, drying, and manufacturing (Won et al., 2010; Won et al., 2012; Brantley et al., 2014a; Gufford et al., 2014b). These challenges in consistency necessitate careful consideration of key individual constituents

prior to synthesis of metabolite standards. In addition, the supply of individual constituents to use as starting materials for the generation of metabolite standards can range from limited to nonexistent, a challenge not frequently encountered when synthesizing a metabolite standard of a conventional small molecule pharmaceutical. Addressing these additional hurdles requires collaboration between the divergent yet complementary skillsets of clinical pharmacologists and natural products chemists. This partnership can unravel the complicated composition and pharmacology of herbal products to improve the understanding of the disposition and action of these products.

Chemoenzymatic generation of major β-glucuronides of the flavonolignans silybin A and silybin B, the primary constituents of the semi-purified milk thistle extract silibinin, has been reported (Kren et al., 2000; Han et al., 2004; Jancova et al., 2011; Kren et al., 2013; Charrier et al., 2014). However, approaches to enhance the efficiency of these procedures remain unexplored. Moreover, the crude milk thistle extract, silymarin, contains at least seven flavonolignan diastereoisomers, including isosilybin A and isosilybin B, which also undergo extensive glucuronidation. Challenges in isolating sufficient quantities of individual parent flavonolignans from silymarin has likely hindered generation of glucuronide metabolites for these structurally-related constituents. Methods to isolate gram quantities of pure flavonolignans, including silybin A, silybin B, isosilybin A, and isosilybin B, have been developed (Graf et al., 2007; Monti et al., 2010). Chemical synthesis of glucuronide conjugates could be pursued but would require synthesis of an extensive library of orthogonally protected precursors of each flavonolignan (Stachulski and Meng, 2013; Zhang et al., 2013). Chemoenzymatic processes using isolated constituents as starting materials, followed by purification and structural characterization using natural products chemistry protocols, can be used to efficiently generate flavonolignan glucuronides on the multi-mg scale.

The cost-effective availability of authentic glucuronide metabolites of herbal product constituents will facilitate evaluation of pharmacologic activity, quantitative assessment of

metabolic clearance pathways, direct quantification in biological matrices to determine systemic exposure, and development of additional assays to describe herbal product constituent disposition. Using milk thistle as the model herbal product, the objective of this work was to generate glucuronides of select flavonolignans to fill multiple knowledge gaps in the understanding of herbal product disposition and action. The aims were to (1) enhance efficiency by optimizing reaction conditions for maximal glucuronide formation and (2) evaluate alternate enzyme and reagent sources to improve cost-effectiveness. Results form the foundation for a systematic approach to synthesize and characterize herbal product metabolites (Fig. 1).

DMD Fast Forward. Published on August 27, 2015 as DOI: 10.1124/dmd.115.066076
This article has not been copyedited and formatted. The final version may differ from this version.

Materials and Methods

Materials and Chemicals

Human liver (pooled from 50 donors, mixed gender) and bovine liver (pooled from 2 donors, mixed gender, >12 months old) microsomes (HLMs and BLMs, respectively) and bovine liver S9 fraction (pooled from 2 donors, mixed gender, >12 months old) were purchased from Xenotech, LLC (Lenexa, KS). Bovine serum albumin (BSA), $MgCl_2$, silibinin, and UDP-glucuronic acid (UDPGA) were purchased from Sigma-Aldrich (St. Louis, MO). Alamethicin was purchased from Cayman Chemical Company (Ann Arbor, MI). The individual milk thistle flavonolignans were purified as described in detail previously (Graf et al., 2007) and were >97% pure as determined by UPLC (Napolitano et al., 2013). Methanol (LC/MS grade), ethanol, Tris-HCl, Tris base, and formic acid were purchased from Fisher Scientific (Waltham, MA). Strata-X 33 µm polymeric reversed phase solid phase extraction columns (60 mg of media each) were purchased from Phenomenex (Torrance, CA). Acetone-d_6 was purchased from Cambridge Isotope Laboratories Inc. (Tewksbury, MA).

Initial Optimization of Conditions

Glucuronidation reaction conditions evaluating a range of microsomal and UDPGA concentrations were examined and compared to typical conditions (Walsky et al., 2012; Walker et al., 2014) to optimize yield and cost. A series of 12 different conditions (Table 1) were examined at six different time points over a 24-h period for silybin A, silybin B, isosilybin A, and isosilybin B. Conditions examined included enzyme source (BLMs vs. S9 fraction), enzyme concentration (1, 0.5, and 0.25 mg/mL for BLMs), and UDPGA concentration relative to flavonolignan concentration (10-fold and 2-fold molar excess). Optimization of alamethicin concentration and source were evaluated as potential cost-saving measures using a series of reactions with varying alamethicin concentration and an in-house alamethicin source (alamethicin F50, which was isolated from a filamentous fungal culture, MSX70741, as detailed previously) (Ayers et al., 2012).

DMD Fast Forward. Published on August 27, 2015 as DOI: 10.1124/dmd.115.066076
This article has not been copyedited and formatted. The final version may differ from this version.

A master mixture of $MgCl_2$, BSA, and alamethicin was prepared in Tris-HCl buffer (100 mM, pH 7.4) at 3-times the final reaction concentration. This mixture was split into two aliquots, and UDPGA was added at either 10- or 2-fold molar excess. Each of these mixtures was split into four aliquots, and the four flavonolignans were added separately from DMSO stock solutions (19.28 mg/mL). Each flavonolignan-containing mixture was divided further into six microcentrifuge tubes. Three different volumes of BLMs (2 mg/mL) or bovine S9 (4 mg/mL) were added, depending on desired concentration, with Tris-HCl buffer added to produce a final reaction volume of 0.65 mL. The 48 mixtures were incubated at 37 °C, after which 100-µL aliquots were removed and quenched with 300 µL of ice-cold MeOH at each time point (0, 2, 4, 8, 12, and 24 h), generating 288 samples, which were stored at 4 °C until analysis.

Samples were prepared for UPLC-MS analysis by centrifugation (15,000 g x 2 min), and 60 µL of the supernatant were removed and mixed with 90 µL of H_2O in a 96-well plate (final concentration of 30% MeOH and 40 µM total flavonolignans). The resultant mixture (3 µL injection volume) was separated using an Acquity UPLC HSS C18 (1.8 µm, 50 × 2.1 mm) column with an Acquity UPLC system (Waters Corp., Milford, MA) coupled to a Q Exactive Plus high-resolution electrospray ionization mass spectrometer (Thermo Fisher Scientific, San Jose, CA) operated in positive mode.

Large Scale Reaction of Silybin A and Purification of Glucuronides

After determining the optimal reaction conditions for silybin A (0.8 mM UDPGA, 0.25 mg/mL BLMs, 37 °C x 12 h), a large scale reaction was initiated. Tris-HCl (204 mL, 100 mM, pH 7.4), $MgCl_2 \cdot 6H_2O$ (212 mg, 5 mM), UDPGA (108 mg, 0.8 mM), BSA (1.05 g, 0.5% w/v), silybin A (40 mg in 1.7 mL DMSO, 0.4 mM), alamethicin (8 mg in 0.4 mL DMSO, 38 µg/mL, 19.5 µM), and BLMs (2.5 mL of 20 mg/mL, 0.25 mg/mL) were combined to yield a total reaction volume of 209 mL (1.0% DMSO final). The reaction was incubated at 37 °C in a rotary incubator at 100 rpm to prevent settling of the BLMs during the incubation and was terminated after 12 h by adding 3 volumes (630 mL) of ice-cold MeOH and stored at 4 °C. The resulting mixture was

DMD Fast Forward. Published on August 27, 2015 as DOI: 10.1124/dmd.115.066076
This article has not been copyedited and formatted. The final version may differ from this version.

filtered (qualitative grade Whatman filter paper in a Büchner funnel), and the supernatant was evaporated to a volume of ~20 mL. Wash solution (10% MeOH) was added to yield a volume of ~50 mL (5% MeOH). The reaction concentrate was purified further using six 60-mg Strata-X cartridges, loading 1 mL at a time over 8 successive purification cycles. Before the first cycle, each cartridge was conditioned with 4 mL of 100% MeOH and equilibrated with 3 mL of 10% MeOH. For each cycle, the cartridges were pre-equilibrated with 3 mL of 10% MeOH, loaded with 1.0 mL of the reaction concentrate, and washed with 3 mL of 10% MeOH; the combined load and wash fractions were designated pool 1. The sample-loaded cartridges were eluted with 3 mL of 50% MeOH, generating pool 2, then eluted with 4 mL of 100% MeOH, generating pool 3. Each of the pools was dried under vacuum, yielding 4,707 mg of pool 1, 51 mg of pool 2, and 24 mg of pool 3.

Pool 2 (a white solid), containing the desired reaction products, was dissolved in 500 µL of 4:1 DMSO:dioxane (producing a fluorescent yellow-green solution) and purified in two successive separations (250 µL each) by preparative reverse phase-HPLC using a Gemini-NX C18 (5 µm, 250 × 21 mm) column with a gradient from 20:80 to 40:60 CH_3CN:H_2O (0.1% formic acid) over 30 min at a flow rate of 21.2 mL/min with peak elution monitored at 288 nm. Separations were accomplished using a Varian ProStar HPLC system (Varian Inc., Palo Alto, CA, USA) equipped with ProStar 210 pumps and a ProStar 335 photodiode array detector and Galaxie Chromatography Workstation (version 1.9.3.2, Varian Inc.).

Characterization and Structural Confirmation

All NMR experiments were conducted in acetone-d_6 using either an Agilent 700 NMR spectrometer equipped with a cryoprobe (700 and 175 MHz for ^{1}H and ^{13}C, respectively; Agilent Technologies, Santa Clara, CA) or a JEOL ECS-400 NMR spectrometer (399.78 MHz for ^{1}H and 100.53 MHz for ^{13}C; JEOL Ltd., Tokyo, Japan) equipped with an auto tune 5 mm field gradient tunable Royal probe (NM-03810RO5/UPG). High resolution electrospray ionization mass spectrometry (HRESIMS) data were collected using an electrospray ionization source

coupled to a Q Exactive Plus system (Thermo Fisher Scientific, San Jose, CA, USA) in positive and negative ionization modes via a liquid chromatography/autosampler system comprised of an Acquity UPLC system (Waters Corp., Milford, MA, USA).

Comparison of BLM versus HLM Generated Glucuronides

Flavonolignan glucuronidation in BLMs was compared to HLMs using the previously determined optimal reaction conditions for silybin A in BLMs (Table 3). A mixture of $MgCl_2$, BSA, alamethicin, and UDPGA was prepared in Tris-HCl buffer (100 mM, pH 7.4) at 2.5-times the final reaction concentration and split into four aliquots. The four flavonolignans were added separately from DMSO stock solutions (19.28 mg/mL) and divided to yield duplicate microcentrifuge tubes. BLMs or HLMs (0.424 mg/mL) in Tris-HCl buffer were added to produce a final reaction volume of 0.65 mL. Final concentrations of all reaction ingredients were the same as those described above for the large scale reaction of silybin A. The 8 mixtures were incubated at 37 °C, after which 100-µL aliquots were removed and quenched with 300 µL of ice-cold MeOH at each time point (0, 2, 4, 8, 12, and 24 h), generating 48 samples, which were stored at 4 °C until analysis. Samples were prepared for and analyzed by UPLC-MS as described above.

DMD Fast Forward. Published on August 27, 2015 as DOI: 10.1124/dmd.115.066076
This article has not been copyedited and formatted. The final version may differ from this version.

Results

Synthesis of authentic glucuronides of herbal products is achievable.

Milk thistle flavonolignans demonstrated compound-dependent glucuronidation (Fig. 2, 3); typically, 3 to 5 glucuronidated products were observed by mass spectrometry for each reaction. Silybin A generated five mono-glucuronides, silybin B generated four mono-glucuronides, isosilybin A generated four mono-glucuronides, and isosilybin B generated three mono-glucuronides (Fig. 2, 3). Di-glucuronide flavonolignans were detected only in trace amounts. Optimization and scaling up of incubation procedures were focused on mono-glucuronide formation due to the paucity of di-glucuronide conjugates. Optimal incubation times based upon maximal product formation (0.8 mM UDPGA) were 8, 8, 4, and 12 hours for silybin A, silybin B, isosilybin A, and isosilybin B, respectively (Fig. 2, 3). Two-fold molar excess of UDPGA and 0.25 mg/mL protein was optimal for all flavonolignans. Only silybin B was conjugated more rapidly by S9 than BLMs, representing a potential cost savings measure for generating silybin B glucuronides.

BLMs represent a cost-effective and efficient system for generating glucuronides.

Optimized reaction conditions required 4-fold less enzyme and 5-fold less UDPGA cofactor compared to standard conditions (Table 1). Use of BLMs and optimized reaction conditions yielded substantial (at least 5-fold) cost savings compared to standard reaction conditions using human-derived subcellular fractions (Table 3). Further cost savings can be realized using an alternate alamethicin source [i.e., alamethicin F50 from fungal culture MSX70741 (Ayers et al., 2012)] for synthetic reactions (~$150 for a 25 mg scale reaction). Relatively low protein concentrations of optimized conditions would be expected to reduce compound loss to non-specific binding and simplify purification procedures.

Large scale generation of glucuronides facilitates structural characterization.

Large scale synthesis generated three glucuronides of silybin A, which were purified by preparative HPLC (Fig. 4A). Compound 1 eluted at 13.5 min (15.7 mg), compound 2 at 15.1 min

DMD Fast Forward. Published on August 27, 2015 as DOI: 10.1124/dmd.115.066076
This article has not been copyedited and formatted. The final version may differ from this version.

(1.6 mg), and compound 3 at 18.5 min (11.1 mg); the weights indicate the amounts isolated based on a reaction that started with 40 mg of silybin A. The purity of the glucuronides was measured by UPLC-MS, and the UV data were indicative of the conjugated core of flavonolignans (Fig. 4B). The structures of the three silybin A glucuronides (**1**-**3**) were assigned primarily using ^{1}H, ^{13}C, correlation spectroscopy (COSY), heteronuclear single quantum correlation (HSQC), and heteronuclear multiple bond correlation (HMBC) NMR data (Table 2, Fig. 5); the data for the major product (compound **1**) are discussed below, and the other glucuronides (compounds **2** and **3**) were assigned in an analogous manner (Supplemental Figs. S1-S6).

The HRESIMS (Fig. 6), ^{13}C NMR (Table 2), and HSQC data for the major product of the silybin A glucuronidation reaction (compound **1** in Figs. 4-7) indicated a molecular formula of $C_{31}H_{30}O_{16}$, suggesting an index of hydrogen deficiency of 17. The ^{1}H NMR spectrum (Fig. S1) of **1** displayed signals for a methoxy group, eight aromatic protons, nine oxymethines, and a pair of non-equivalent protons for the oxymethylene group, while the ^{13}C NMR spectrum revealed 31 carbons (20 sp^2 [eight protonated] and 11 sp^3 [nine tertiary, one secondary, and 1 primary]). Two 1,2,4-trisubstituted aromatic rings were identified based on ^{1}H-^{1}H coupling constants ($^{2}J_{H,H}$=8.3 Hz, and $^{4}J_{H,H}$=1.8 Hz), and the corresponding ^{13}C NMR shifts (δ_C 144.7, 145.2, 148.5, and 148.0 for C-3′, C-4′, C-3′′, and C-4′′, respectively) required that they each be 1,2-dioxygenated. An additional tetrasubstituted aromatic ring, which was 1,3,5-trioxygenated, also was observed. Finally, two carbonyl carbons (δ_C 199.0 and 170.0 for C-4 and C-7′′′, respectively) accounted for the remaining sp^2 carbons.

The structure of the silybin A portion of **1** was established by 1D and 2D-NMR data and through comparisons to the literature (Lee and Liu, 2003). The structural data from the ^{1}H NMR spectrum of **1** (Table 2; Fig. S1) were consistent with the characteristics of a 5,7-dioxygenated flavanonol by the signals at δ_H 6.20 (1H, s, H-6), 6.20 (1H, s, H-8), 5.18 (1H, d, J = 11.7 Hz, H-2), and 4.75 (1H, d, J = 11.7 Hz, H-3). The aromatic proton signals at δ_H 7.17 (1H, d, J = 1.8 Hz,

DMD Fast Forward. Published on August 27, 2015 as DOI: 10.1124/dmd.115.066076
This article has not been copyedited and formatted. The final version may differ from this version.

H-2′), 6.97(1H, d, *J* = 8.3 Hz, H-5′), and 7.10 (1H, dd, *J* = 8.3, 1.8 Hz, H-6′) could be attributed to the B-ring unit of silybin A. The aromatic proton signals at δ_H 7.15 (1H, d, *J* = 1.8 Hz, H-2′′), 6.88 (1H, d, *J* = 8.3 Hz, H-5′′), and 6.98 (1H, dd, *J* = 8.3, 1.8 Hz, H-6′′) could be attributed to the E-ring unit of silybin A. The proton signals at δ_H 5.01 (1H, d, *J* = 8.3 Hz, H-7′′), δ_H 4.17 (1H, ddd, *J* = 8.3, 4.4, 2.4 Hz, H-8′′), δ_H 3.76 (1H, dd, *J* = 12.4, 2.4 Hz, H-9′′a), and δ_H 3.52 (1H, dd, *J* = 12.4, 4.4 Hz, H-9′′b) along with the aromatic proton signals for the E-ring unit could be attributed to the coniferyl alcohol moiety of silybin A.

Additional proton (5 oxymethines) and carbon signals in the spectra of **1** indicated condensation of silybin A with a glucuronide moiety. The anomeric H-1′′′ of the glucuronide portion of **1** was readily identifiable due to its chemical shift, coupling pattern, and coupling constant (δ_H 5.27, d, 7.8 Hz). The two main structural units of **1** were linked on the basis of an HMBC correlation of H-1′′′ to C-7 (Figs. 5, 6, S2). The presence of a sharp peak at approximately δ_H 11.5, due to intramolecular H-bonding between the phenolic proton at C-5 to the C-4 carbonyl, further verified the linkage at the C-7 position.

The structures of compounds **2** and **3** were elucidated in a similar manner (Figs. 6, S3-S6; Table 2). With respect to the characterization of flavonolignans by NMR, in general (Napolitano et al., 2013), this study varied in one major aspect. Based on earlier research that derivatized the flavonolignans (Sy-Cordero et al., 2012; Althagafy et al., 2013), the phenol moieties were hypothesized to be glucuronidated readily; indeed, other researchers have reported this observation (Kren et al., 2000; Jancova et al., 2011; Kren et al., 2013; Charrier et al., 2014). Determining the position of glucuronidation required an HMBC correlation from the anomeric proton back to the carbon attached to the phenol (Fig. 6). However, such a correlation would be somewhat inconclusive if the phenolic protons at the non-glucuronidated positions were not observed, which was a challenge at the 5 position due to chelation with the carbonyl and proton exchange in protic solvents, e.g. MeOH-d_4. Thus, all NMR spectra were acquired in acetone-d_6 such that the phenolic protons could be observed readily. For compounds **2** and **3**,

DMD Fast Forward. Published on August 27, 2015 as DOI: 10.1124/dmd.115.066076
This article has not been copyedited and formatted. The final version may differ from this version.

the ^{13}C NMR data (Figs. S3, S5; Table 2) displayed 31 signals, which were six more than silybin A due to the resonances from the glucuronic acid motif at C-1´´´ through C-7´´´. The anomeric C-1´´´appeared at approximately δ_C 102 and the anomeric H-1´´´at approximately δ_H 5.0 as a doublet with a coupling constant at approximately 7 Hz, characteristic of the β-anomer (Pearson et al., 2005; Walker et al., 2007). Data from the HMBC experiments (Figs. S4, S6) demonstrated the connectivity of the glucuronide moiety, where correlations were observed between H-1´´´ to C-5 and H-1´´´ to C-4´´ for **2** and **3**, respectively.

BLMs generate human-relevant glucuronides with enhanced efficiency.

Compared to HLMS, BLMs converted all four flavonolignans to their respective glucuronides more rapidly and completely (Fig. 8). Silybin A and silybin B glucuronides were produced similarly by both BLMs and HLMs. The predominant glucuronides of isosilybin A and isosilybin B generated using BLMs (elution time 3.1 min) were opposite of the predominant glucuronides generated using HLMs (elution time 2.8 min) (Fig. 8). Overall, BLMs generated glucuronide profiles were similar to those generated by HLMs (Fig. 8).

Discussion

Partnerships between clinical pharmacologists and natural products chemists with divergent yet complementary skillsets are imperative to advance the understanding of herbal product constituent disposition and pharmacology. Complete characterization of herbal product metabolites will enable identification of sites of metabolic lability that could be targeted to optimize pharmacokinetics of therapeutically promising constituents. These studies would enable structure-activity relationships that lay the groundwork for application of rational drug design concepts to compounds of natural origin.

Metabolite characterization can identify the potential for bioactivation and toxicity of a molecule that may occur in vivo. Identifying and characterizing metabolites with appreciable human exposure is critical to a complete understanding of the pharmacology of a particular herbal product. Minor metabolites also may be important to overall activity, as they can be unique in both disposition and action. Individual constituents within complex herbal product mixtures can be differentially metabolized. Milk thistle flavonolignans, although structurally similar (i.e., constitutional isomers), exemplify this consideration, as evidenced by the in vitro depletion curves demonstrating compound-dependent metabolism in BLMs (Figs. 2, 3) and differential metabolism in BLMs compared to HLMs (Fig. 8). Although evaluation of isolated constituents can simplify investigation, the possibility exists that one constituent may modulate metabolism of another both in vitro and in vivo. This possibility underscores the importance of evaluating both individual constituents and complex mixtures to ascertain the metabolic fates in each scenario; such experiments would be exceedingly difficult without the availability of authentic metabolite standards.

Typical chemoenzymatic glucuronidation reactions include a ten-fold molar excess of UDPGA and ≥1 mg/mL of microsomal protein. Saturating UDPGA concentrations (5-10 mM) are routinely employed when recovering in vitro kinetic parameters using HLMs (K_m ~ 0.2-1.3 mM) (Court et al., 2001) to eliminate UDPGA availability as a potential rate-limiting step. Application

DMD Fast Forward. Published on August 27, 2015 as DOI: 10.1124/dmd.115.066076
This article has not been copyedited and formatted. The final version may differ from this version.

of these relatively high concentrations to synthetic reactions assumes that excess co-factor and enzyme enhance yield. The current work demonstrated that using less of these reagents for chemoenzymatic synthesis is an effective cost-saving measure and that excess enzyme and reagents can reduce yields via what appear to be reverse catalases. Saccharolactone, a β-glucuronidase inhibitor, often is added to microsomal incubations to prevent enzymatic degradation of glucuronides. However, hepatic microsomal preparations are not expected to be substantially impacted by adding saccharolactone (Oleson and Court, 2008), and degradation of glucuronides under optimized conditions was minimal (Fig. 2). Consequently, saccharolactone was not included in the optimized reaction. Detergents could be explored as an additional cost savings measure to replace alamethicin, but the impact of detergent selection and concentration on glucuronide yield would need to be evaluated (Soars et al., 2003). Albumin was added to all microsomal incubations based upon reports of substrate-dependent decreases in K_m and increases in V_{max} (Rowland et al., 2008; Manevski et al., 2011; Gill et al., 2012; Walsky et al., 2012; Manevski et al., 2013), which are believed to reflect binding to inhibitory fatty acids (Rowland et al., 2007). Selection of additives that can modulate microsomal UGT activity is an important consideration that can be addressed in microscale optimization reactions prior to scaling up synthetic procedures.

Generation of flavonolignan glucuronides on the desired scale appeared initially to be overtly cost-prohibitive based on literature protocols. However, relatively inexpensive micro-scale optimization reduced the total costs by at least an order of magnitude, making these previously cost-prohibitive experiments (thousands of US dollars per reaction) feasible (Table 3). Cost-effective generation of large (multi-mg) quantities are needed to support detailed investigation of the kinetics and pharmacology of herbal product metabolites across multiple laboratories. However, cost savings could be realized with micro scale (<1 mg) incubations followed by quantitative NMR to generate small, yet useful, quantities of metabolites using approaches similar to those described for the synthesis of drug metabolites (Walker et al., 2011;

Walker et al., 2014). Flavonolignan cost was not factored into total cost estimates, as these compounds are isolated in-house, precluding meaningful comparisons to alternate herbal product constituents that can vary widely in cost and availability. Synthetic processes using isolated constituent starting materials enhances optimization of specific reaction conditions and simplifies metabolite purification, leading to enhanced yield. Enhanced efficiency is crucial to reduce waste of limited individual constituents that may take weeks to months to isolate and purify in quantities sufficient for metabolite synthesis. Deconvolution of complex parent and metabolite mixtures encountered in both in vitro and clinical samples can be overcome partially using isolated constituents to simplify the diversity of generated metabolites in a particular system.

Bioanalysis of herbal product glucuronides historically has relied on indirect methods using enzymatic (e.g., β-glucuronidase) incubations to cleave the conjugates, followed by analysis of the parent compound. Indirect quantification methods increase sample preparation time and frequently are plagued by poor accuracy and reproducibility resulting from incomplete enzymatic hydrolysis and instability of metabolites under enzymatic conditions. Moreover, simultaneous cleavage of multiple glucuronides present in a given system precludes quantitative description of individual glucuronides. Lack of commercially available glucuronide standards necessitates chemoenzymatic synthesis and purification of glucuronide metabolites for analytical development and application. The reaction scales described in the current work are capable of supporting bioanalytical method development, metabolism inquiries, and pharmacology evaluations.

In summary, techniques to efficiently and cost-effectively generate and purify authentic glucuronide metabolites of a model herbal product have been developed (Fig. 1). This approach was bolstered by a partnership between clinical pharmacology and natural products chemistry expertise. These techniques are essential to improve the understanding of mechanisms underlying herbal product disposition and action. Authentic metabolites can be used to provide

quantitative description of metabolite formation rates, exposure, and activity. Quantitative description of herbal product disposition and action could lead to improved translation of natural product discoveries from bench to bedside.

Acknowledgements

M.F.P. dedicates this article to Dr. David P. Paine. We thank Dr. Cedric Pearce of Mycosynthetix, Inc. for access to fungal culture MSX70741 and Dr. Daneel Ferreira of the University of Mississippi for helpful discussions.

Authorship Contributions

Participated in research design: Gufford, Graf, Oberlies, Paine

Conducted experiments: Gufford, Graf, Paguigan

Contributed new reagents or analytical tools: Graf, Oberlies

Performed data analysis: Gufford, Graf, Paguigan, Oberlies, Paine

Wrote or contributed to writing of the manuscript: Gufford, Graf, Paguigan, Oberlies, Paine

References

Abenavoli L, Capasso R, Milic N, and Capasso F (2010) Milk thistle in liver diseases: past, present, future. *Phytother Res* **24:**1423-1432.

Althagafy HS, Graf TN, Sy-Cordero AA, Gufford BT, Paine MF, Wagoner J, Polyak SJ, Croatt MP, and Oberlies NH (2013) Semisynthesis, cytotoxicity, antiviral activity, and drug interaction liability of 7-O-methylated analogues of flavonolignans from milk thistle. *Bioorg Med Chem* **21:**3919-3926.

Ayers S, Ehrmann BM, Adcock AF, Kroll DJ, Carcache de Blanco EJ, Shen Q, Swanson SM, Falkinham JO, 3rd, Wani MC, Mitchell SM, Pearce CJ, and Oberlies NH (2012) Peptaibols from two unidentified fungi of the order Hypocreales with cytotoxic, antibiotic, and anthelmintic activities. *J Pept Sci* **18:**500-510.

Brantley SJ, Argikar AA, Lin YS, Nagar S, and Paine MF (2014a) Herb-drug interactions: challenges and opportunities for improved predictions. *Drug Metab Dispos* **42:**301-317.

Brantley SJ, Graf TN, Oberlies NH, and Paine MF (2013) A systematic approach to evaluate herb-drug interaction mechanisms: investigation of milk thistle extracts and eight isolated constituents as CYP3A inhibitors. *Drug Metab Dispos* **41:**1662-1670.

Brantley SJ, Gufford BT, Dua R, Fediuk DJ, Graf TN, Scarlett YV, Frederick KS, Fisher MB, Oberlies NH, and Paine MF (2014b) Physiologically based pharmacokinetic modeling framework for quantitative prediction of an herb-drug interaction. *CPT Pharmacometrics Syst Pharmacol* **3:**e107.

Brantley SJ, Oberlies NH, Kroll DJ, and Paine MF (2010) Two flavonolignans from milk thistle (Silybum marianum) inhibit CYP2C9-mediated warfarin metabolism at clinically achievable concentrations. *J Pharmacol Exp Ther* **332:**1081-1087.

Charrier C, Azerad R, Marhol P, Purchartová K, Kuzma M, and Křen V (2014) Preparation of silybin phase II metabolites: Streptomyces catalyzed glucuronidation. *Journal of Molecular Catalysis B: Enzymatic* **102:**167-173.

Court MH, Duan SX, von Moltke LL, Greenblatt DJ, Patten CJ, Miners JO, and Mackenzie PI (2001) Interindividual variability in acetaminophen glucuronidation by human liver microsomes: identification of relevant acetaminophen UDP-glucuronosyltransferase isoforms. *J Pharmacol Exp Ther* **299:**998-1006.

Di L and Obach RS (2015) Addressing the Challenges of Low Clearance in Drug Research. *AAPS J*.

Gill KL, Houston JB, and Galetin A (2012) Characterization of in vitro glucuronidation clearance of a range of drugs in human kidney microsomes: comparison with liver and intestinal glucuronidation and impact of albumin. *Drug Metab Dispos* **40:**825-835.

Graf TN, Wani MC, Agarwal R, Kroll DJ, and Oberlies NH (2007) Gram-scale purification of flavonolignan diastereoisomers from Silybum marianum (Milk Thistle) extract in support of preclinical in vivo studies for prostate cancer chemoprevention. *Planta Med* **73:**1495-1501.

Gufford BT, Chen G, Lazarus P, Graf TN, Oberlies NH, and Paine MF (2014a) Identification of diet-derived constituents as potent inhibitors of intestinal glucuronidation. *Drug Metab Dispos* **42:**1675-1683.

Gufford BT, Chen G, Vergara AG, Lazarus P, Oberlies NH, and Paine MF (2015) Milk Thistle Constituents Inhibit Raloxifene Intestinal Glucuronidation: A Potential Clinically Relevant Natural Product-Drug Interaction. *Drug Metab Dispos* **43:**1353-1359.

Gufford BT, Lazarus P, Oberlies NH, and Paine MF (2014b) Predicting Pharmacokinetic Herb-Drug Interactions: Overcoming Hurdles That Extend beyond Drug-Drug Interactions. *AAPS Newsmagazine***:**19-22.

Gurley BJ (2012) Pharmacokinetic herb-drug interactions (part 1): origins, mechanisms, and the impact of botanical dietary supplements. *Planta Med* **78:**1478-1489.

Gurley BJ, Barone GW, Williams DK, Carrier J, Breen P, Yates CR, Song PF, Hubbard MA, Tong Y, and Cheboyina S (2006) Effect of milk thistle (Silybum marianum) and black cohosh (Cimicifuga racemosa) supplementation on digoxin pharmacokinetics in humans. *Drug Metab Dispos* **34:**69-74.

Gurley BJ, Fifer EK, and Gardner Z (2012) Pharmacokinetic herb-drug interactions (part 2): drug interactions involving popular botanical dietary supplements and their clinical relevance. *Planta Med* **78:**1490-1514.

Han YH, Lou HX, Ren DM, Sun LR, Ma B, and Ji M (2004) Stereoselective metabolism of silybin diastereoisomers in the glucuronidation process. *J Pharm Biomed Anal* **34:**1071-1078.

Jancova P, Siller M, Anzenbacherova E, Kren V, Anzenbacher P, and Simanek V (2011) Evidence for differences in regioselective and stereoselective glucuronidation of silybin diastereomers from milk thistle (Silybum marianum) by human UDP-glucuronosyltransferases. *Xenobiotica* **41:**743-751.

Kren V, Marhol P, Purchartova K, Gabrielova E, and Modriansky M (2013) Biotransformation of silybin and its congeners. *Curr Drug Metab* **14:**1009-1021.

Kren V, Ulrichova J, Kosina P, Stevenson D, Sedmera P, Prikrylova V, Halada P, and Simanek V (2000) Chemoenzymatic preparation of silybin beta-glucuronides and their biological evaluation. *Drug Metab Dispos* **28:**1513-1517.

Lee DY and Liu Y (2003) Molecular structure and stereochemistry of silybin A, silybin B, isosilybin A, and isosilybin B, Isolated from Silybum marianum (milk thistle). *J Nat Prod* **66:**1171-1174.

Lindstrom A, Ooyen C, Lynch M, Blumenthal M, and Kawa K (2014) Sales of herbal dietary supplements increase by 7.9% in 2013, marking a decade of rising sales: turmeric supplements climb to top ranking in natural channel. *HerbalGram***:**52-56.

Loguercio C and Festi D (2011) Silybin and the liver: from basic research to clinical practice. *World J Gastroenterol* **17:**2288-2301.

Manevski N, Moreolo PS, Yli-Kauhaluoma J, and Finel M (2011) Bovine serum albumin decreases Km values of human UDP-glucuronosyltransferases 1A9 and 2B7 and increases Vmax values of UGT1A9. *Drug Metab Dispos* **39:**2117-2129.

Manevski N, Troberg J, Svaluto-Moreolo P, Dziedzic K, Yli-Kauhaluoma J, and Finel M (2013) Albumin stimulates the activity of the human UDP-glucuronosyltransferases 1A7, 1A8, 1A10, 2A1 and 2B15, but the effects are enzyme and substrate dependent. *PLoS One* **8:**e54767.

Monti D, Gazak R, Marhol P, Biedermann D, Purchartova K, Fedrigo M, Riva S, and Kren V (2010) Enzymatic kinetic resolution of silybin diastereoisomers. *J Nat Prod* **73:**613-619.

Napolitano JG, Lankin DC, Graf TN, Friesen JB, Chen SN, McAlpine JB, Oberlies NH, and Pauli GF (2013) HiFSA fingerprinting applied to isomers with near-identical NMR spectra: the silybin/isosilybin case. *J Org Chem* **78:**2827-2839.

Oleson L and Court MH (2008) Effect of the beta-glucuronidase inhibitor saccharolactone on glucuronidation by human tissue microsomes and recombinant UDP-glucuronosyltransferases. *J Pharm Pharmacol* **60:**1175-1182.

Pearson AG, Kiefel MJ, Ferro V, and von Itzstein M (2005) Towards the synthesis of aryl glucuronides as potential heparanase probes. An interesting outcome in the glycosidation of glucuronic acid with 4-hydroxycinnamic acid. *Carbohydr Res* **340:**2077-2085.

Polyak SJ, Ferenci P, and Pawlotsky JM (2013a) Hepatoprotective and antiviral functions of silymarin components in hepatitis C virus infection. *Hepatology* **57:**1262-1271.

Polyak SJ, Oberlies NH, Pecheur EI, Dahari H, Ferenci P, and Pawlotsky JM (2013b) Silymarin for HCV infection. *Antivir Ther* **18:**141-147.

Rowland A, Gaganis P, Elliot DJ, Mackenzie PI, Knights KM, and Miners JO (2007) Binding of inhibitory fatty acids is responsible for the enhancement of UDP-glucuronosyltransferase 2B7 activity by albumin: implications for in vitro-in vivo extrapolation. *J Pharmacol Exp Ther* **321:**137-147.

Rowland A, Knights KM, Mackenzie PI, and Miners JO (2008) The "albumin effect" and drug glucuronidation: bovine serum albumin and fatty acid-free human serum albumin enhance the glucuronidation of UDP-glucuronosyltransferase (UGT) 1A9 substrates but not UGT1A1 and UGT1A6 activities. *Drug Metab Dispos* **36:**1056-1062.

Soars MG, Ring BJ, and Wrighton SA (2003) The effect of incubation conditions on the enzyme kinetics of udp-glucuronosyltransferases. *Drug Metab Dispos* **31:**762-767.

Stachulski AV and Meng X (2013) Glucuronides from metabolites to medicines: a survey of the in vivo generation, chemical synthesis and properties of glucuronides. *Nat Prod Rep* **30:**806-848.

Sy-Cordero AA, Graf TN, Runyon SP, Wani MC, Kroll DJ, Agarwal R, Brantley SJ, Paine MF, Polyak SJ, and Oberlies NH (2012) Enhanced bioactivity of silybin B methylation products. *Bioorg Med Chem*.

Walker GS, Atherton J, Bauman J, Kohl C, Lam W, Reily M, Lou Z, and Mutlib A (2007) Determination of degradation pathways and kinetics of acyl glucuronides by NMR spectroscopy. *Chem Res Toxicol* **20:**876-886.

Walker GS, Bauman JN, Ryder TF, Smith EB, Spracklin DK, and Obach RS (2014) Biosynthesis of drug metabolites and quantitation using NMR spectroscopy for use in pharmacologic and drug metabolism studies. *Drug Metab Dispos* **42:**1627-1639.

Walker GS, Ryder TF, Sharma R, Smith EB, and Freund A (2011) Validation of isolated metabolites from drug metabolism studies as analytical standards by quantitative NMR. *Drug Metab Dispos* **39:**433-440.

Walsky RL, Bauman JN, Bourcier K, Giddens G, Lapham K, Negahban A, Ryder TF, Obach RS, Hyland R, and Goosen TC (2012) Optimized assays for human UDP-glucuronosyltransferase (UGT) activities: altered alamethicin concentration and utility to screen for UGT inhibitors. *Drug Metab Dispos* **40:**1051-1065.

Wellington K and Jarvis B (2001) Silymarin: a review of its clinical properties in the management of hepatic disorders. *BioDrugs* **15:**465-489.

Won CS, Oberlies NH, and Paine MF (2010) Influence of dietary substances on intestinal drug metabolism and transport. *Curr Drug Metab* **11:**778-792.

Won CS, Oberlies NH, and Paine MF (2012) Mechanisms underlying food-drug interactions: inhibition of intestinal metabolism and transport. *Pharmacol Ther* **136:**186-201.

Zhang M, Jagdmann GE, Jr., Van Zandt M, Sheeler R, Beckett P, and Schroeter H (2013) Chemical synthesis and characterization of epicatechin glucuronides and sulfates: bioanalytical standards for epicatechin metabolite identification. *J Nat Prod* **76:**157-169.

Footnotes

a. This work was supported by the National Institutes of Health National Institute of General Medical Sciences [Grant R01 GM077482-S1]. B.T.G. was supported by fellowships awarded by the American Foundation for Pharmaceutical Education and the James and Diann Robbers Student Research Fund. B.T.G. is currently supported by the National Institute of General Medical Sciences [Grant T32 GM008425]. Alamethicin F50 was isolated as part of Program Project Grant P01 CA125066 from the National Institutes of Health National Cancer Institute. The content is solely the responsibility of the authors and does not necessarily represent the official views of the National Institute of General Medical Sciences or the National Institutes of Health.

b. Reprint requests: Mary F. Paine, RPh, PhD

PBS 341, PO Box 1495

College of Pharmacy

Washington State University

Spokane, WA 99210-1495

Office: (509) 358-7759

Fax: (509) 368-6561

Email: mary.paine@wsu.edu

DMD Fast Forward. Published on August 27, 2015 as DOI: 10.1124/dmd.115.066076
This article has not been copyedited and formatted. The final version may differ from this version.

Figure Legends

Fig. 1. Schematic of proposed approach to generate and characterize authentic herbal product glucuronides.

Fig. 2. Optimization of incubation time, UDPGA concentration, and BLM concentration. Silybin A (**A**), silybin B (**B**), isosilybin A (**C**), or isosilybin B (**D**) (0.4 mM) were incubated with 1 (black), 0.5 (dashed), or 0.25 (crimson) mg/mL BLMs with 4 (upper) or 0.8 (lower) mM UDPGA. Disappearance of flavonolignan starting material (left column) and appearance of glucuronides (right column) were monitored over time. Glucuronide data are presented as the sum of all monoglucuronide products formed at each time point.

Fig. 3. Optimization of incubation time, UDPGA concentration, and S9 concentration. Silybin A (**A**), silybin B (**B**), isosilybin A (**C**), or isosilybin B (**D**) (0.4 mM) was incubated with 2 (gray), 1 (dashed), or 0.5 (black) mg/mL S9 with 4 (upper) or 0.8 (lower) mM UDPGA. Disappearance of flavonolignan starting material (left column) and appearance of glucuronides (right column) were monitored over time. Flavonolignan disappearance and glucuronide formation data using BLMs (0.25 mg/mL) are included as a comparison to microsomal systems (crimson). Glucuronide data are presented as the sum of all monoglucuronide products formed at each time point.

Fig. 4. Analysis of the large scale reaction for silybin A. (**A**) Purification of silybin A glucuronides. Preparative HPLC UV trace (288 nm) of the reaction mixture applied to a Gemini-NX C18 column eluted using a 20-40% gradient of CH_3CN/H_2O (0.1% formic acid). Isolated silybin A glucuronides (**1-3**) are indicated in the chromatogram. (**B**) Stacked plots showing the SIC (left), UV absorbance at 288 nm (middle), and UV spectrum from 190-500 nm (right) of isolated compounds silybin A-7-*O*-β-D-glucuronide (**1**), silybin A-5-*O*-β-D-glucuronide (**2**), and silybin A-4´´-*O*-β-D-glucuronide (**3**).

Fig. 5. Selected HMBC spectrum of **1** (700 MHz/175 MHz) in CD_3OD. The HMBC correlation from H-1‴ to C-7 supports the assigned site of attachment of the glucuronic acid to silybin A.

Fig. 6. Stacked plots showing the HRESIMS for positive (left) and negative (right) ionization modes of isolated compounds silybin A-7-*O*-β-D-glucuronide (**1**), silybin A-5-*O*-β-D-glucuronide (**2**), and silybin A-4´´-*O*-β-D-glucuronide (**3**). Values in parentheses represent the difference between the measured versus calculated mass for the indicated molecular formula; values within 5 ppm are considered valid.

Fig. 7. Structures and diagnostic HMBC correlations of silybin A glucuronides (**1-3**).

Fig. 8. Comparison of BLM versus HLM generated glucuronides. Silybin A (**A**), silybin B (**B**), isosilybin A (**C**), or isosilybin B (**D**) (0.4 mM) were incubated with 0.25 mg/mL BLMs (crimson) or HLMs (black) with 0.8 mM UDPGA. **Left panel.** Disappearance of flavonolignan starting material (dashed lines) and appearance of glucuronides (solid lines) were monitored over time (left). Glucuronide data are presented as the sum of all monoglucuronide products formed at each time point. **Right panel.** UPLC-MS chromatograms of flavonolignan glucuronides (659 m/z) generated following 12 hour incubation with BLMs (upper) or HLMs (lower).

DMD Fast Forward. Published on August 27, 2015 as DOI: 10.1124/dmd.115.066076
This article has not been copyedited and formatted. The final version may differ from this version.

Table 1. Comparison between typical and screened reaction conditions to optimize cost, efficiency, and yield of milk thistle glucuronides.

Reagent	Typical condition[a]	Screened condition(s)
Tris-HCl (pH 7.4) (mM)[b]	100	100
$MgCl_2$ (mM)[b]	5	5
BSA (%, w/v)[b]	0.5	0.5
Alamethicin (μM)[b]	25	25
Silybin A (mM)[b]	0.4	0.4
UDPGA (mM)	4.0	4.0, 0.8
Enzyme source	HLMs	BLMs, bovine S9 fraction
Enzyme source concentration (mg/mL protein)	1.00	1.00, 0.50, 0.25 (BLMs) 2.00, 1.00, 0.50 (S9)

[a]Walker et al. (2014) *Drug Metab Dispos* **42:**1627-1639
[b]Concentration not varied to limit experimental complexity.
BSA, bovine serum albumin; UDPGA, uridine diphosphate glucuronic acid; BLM, bovine liver microsome

DMD Fast Forward. Published on August 27, 2015 as DOI: 10.1124/dmd.115.066076
This article has not been copyedited and formatted. The final version may differ from this version.

Table 2. NMR spectroscopic data for silybin A glucuronides (**1-3**) in acetone-d_6.

	Silybin A-7- *O-ß*-D-glucuronide **1**[a]			Silybin A-5- *O-ß*-D-glucuronide **2**[b*]			Silybin A-4´´- *O-ß*-D-glucuronide **3**[a]		
Position	**δ C**	**δ H (mult, *J* in Hz)**	**HMBC**	**δ C**	**δ H (mult, *J* in Hz)**	**HMBC**	**δ C**	**δ H (mult, *J* in Hz)**	**HMBC**
2	84.2	5.18 d 11.7	3, 4, 8a, 1´, 2´	83.2	5.02 d 11.6	3, 4, 1´, 2´, 6´	84.1	5.11 d 11.5	3, 4, 8a, 1´, 2´, 6´
3	73.1	4.75 d 11.7	2, 4,1´	73.8	4.42 d 11.6	2, 4, 1´	73.0	4.69 d 11.5	2, 4, 1´
4	199.0			192.8			198.2		
4a	103.0			104.2			101.5		
5	164.3			161.3			165.0		
6	97.8	6.20 s	4, 8, 4a, 8a	100.6	6.84 bs	5, 7, 8, 4a	97.1	6.00 d 1.8	4a , 5, 7, 8,
7	166.6			166.8			167.8		
8	96.4	6.20 s	5, 6, 7	98.8	6.03 d 1.8	6, 7, 4a, 8a	96.0	5.96 d 1.8	4, 4a, 6, 7, 8a
8a	163.8			165.0			164.0		
1´	130.9			131.1			131.1		
2´	117.5	7.17 d 1.8	2, 4´, 6´	117.1	7.11 d 1.9	2, 4´	117.4	7.17 d 1.8	2, 4´, 6´
3´	144.7			144.4			144.5		
4´	145.2			144.8			145.1		
5´	117.4	6.97 d 8.3	1´, 2´, 3´	117.3	6.96 d 8.3	1´, 3´	117.4	6.97 d 8.3	1´, 3´
6´	122.2	7.10 dd 8.3, 1.8	2, 2´, 4´	121.9	6.91 dd 8.3, 1.9	4´	122.2	7.1 dd 8.3, 1.8	2, 4´, 5´
1´´	129.1			128.9			132.6		
2´´	111.8	7.15 d 1.8	4´´, 6´´, 7´´	111.9	7.11 d 1.9	4´´, 6´´, 7´´	113.0	7.2 d 1.8	4´´, 6´´, 7´´
3´´	148.5			148.5			150.9		
3´´-OMe	56.3	3.87 s	3´´	56.2	3.83 s	3´´	56.4	3.86 s	3´´
4´´	148.0			147.8			147.8		
5´´	115.7	6.88 d 8.3	1´´, 2´´, 3´´	115.7	6.86 d 8.1	1´´, 3´´	117.4	7.23 d 8.3	1´´, 3´´
6´´	121.6	6.98 dd 8.3, 1.8	2´´, 3´´, 7´´	121.3	6.93 dd 8.1, 1.8	2´´, 4´´, 7´´	121.0	7.06 dd 8.3, 1.8	2´´, 4´´, 7´´
7´´	77.2	5.01 d 8.3	3´, 2´´, 6´´, 8´´, 9´´	77.0	4.95 d 8.1	1´´, 2´´, 6´´, 8´´	76.9	5.06 d 7.8	1´´, 2´´, 6´´, 8´´
8´´	79.5	4.17 ddd 8.3, 4.4, 2.4	7´´	79.2	4.14 ddd 8.1, 4.4, 2.6	7´´	79.4	4.18 ddd 7.8, 3.8, 1.9	7´´
9´´a	61.8	3.76 dd 12.4, 2.4	7´´, 8´´	61.4	3.68 dd 12.2, 2.6	7´´	61.7	3.77 dd 12.4, 1.9	7´´, 8´´
9´´b		3.52 dd 12.4, 4.4	4´		3.48 dd 12.2, 4.4	7´´		3.52 dd 12.4, 3.8	
1´´´	100.6	5.27 d 7.8	7, 5´´´	104.2	4.78 d 7.8	5	102.1	5.16 d 7.3	4´´
2´´´	74.0	3.53 dd 9.4, 7.8	1´´´, 3´´´	73.7	3.50 m	3´´´	74.4	3.59 dd 8.9, 7.3	1´´´, 3´´´
3´´´	76.9	3.61 dd 9.4, 9.0	1´´´, 2´´´, 4´´´	77.0	3.56 m	4´´´	77.2	3.60 dd 9.4, 8.9	2´´´
4´´´	72.4	3.71 dd 9.6, 9.0	3´´´, 7´´´	73.9	3.60 m	3´´´, 1´´´	72.6	3.71 dd 9.6, 9.4	3´´´
5´´´	76.0	4.23 d 9.6	1´´´, 3´´´, 4´´´, 7´´´	--	--		76.1	4.09 d 9.6	1´´´, 3´´´, 4´´´, 7´´´
7´´´	170.0			174.8			170.1		

[a] ^{1}H NMR at 400 MHz and ^{13}C NMR at 100 MHz
[b] ^{1}H NMR at 700 MHz and ^{13}C NMR at 175 MHz; *NMR acquired in 10% D_2O in acetone-d_6
HMBC, heteronuclear multiple bond correlation; δ in ppm

DMD Fast Forward. Published on August 27, 2015 as DOI: 10.1124/dmd.115.066076
This article has not been copyedited and formatted. The final version may differ from this version.

Table 3. Summary of optimal reaction conditions and projected cost savings to generate milk thistle flavonolignan glucuronides.

	Optimized Conditions				**Typical Conditions[a]**
Compound	Silybin A	Silybin B	Isosilybin A	Isosilybin B	N/A
Enzyme source	BLMs	S9	BLMs	BLMs	HLMs
Enzyme concentration (mg/mL)	0.25	0.25	0.25	0.25	1.0
UDPGA (mM)	0.8	0.8	0.8	0.8	4
Time (h)	8	8	4	12	N/A
Cost (USD)[b]	480	310	460	480	2,400

[a]Walker et al. (2014) *Drug Metab Dispos* **42:**1627-1639
[b]based on a 25 mg scale reaction
BLMs, bovine liver microsomes; S9, bovine liver S9 fraction; HLMs, human liver microsomes; UDPGA, uridine diphosphate glucuronic acid

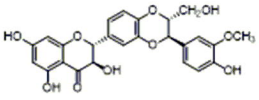

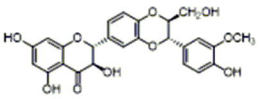

Identify, Isolate, and Purify Herbal Product Constituents

DMD Fast Forward. Published on August 27, 2015 as DOI: 10.1124/dmd.1

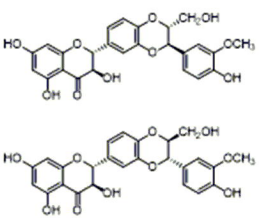

Enzyme
Cofactor
Additives
Incubation Time

Maximal Product Yield

Optimize Reaction Conditions

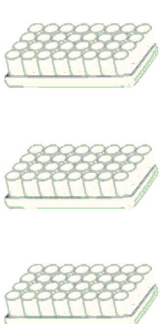

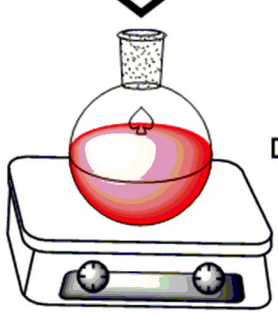

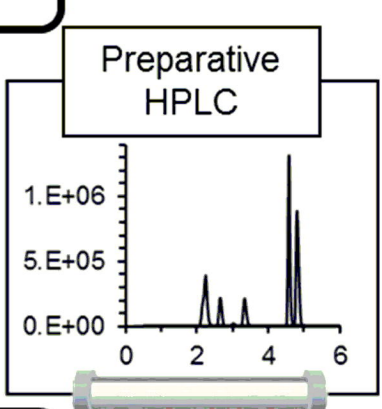

Scale-up Reactions and Purification

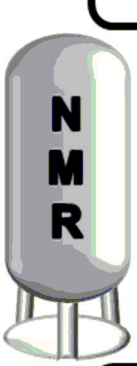

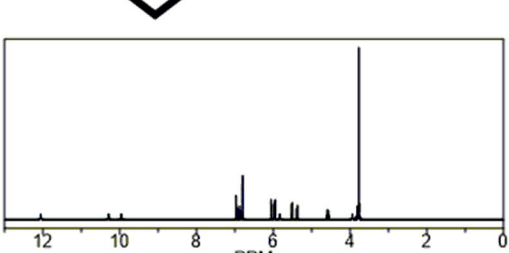

Characterize Products and Confirm Structure

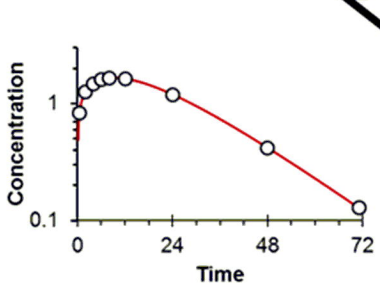

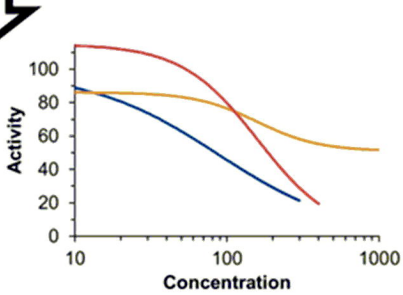

Metabolite PK Metabolite PD

Applications

Figure 1

DMD Fast Forward. Published on August 27, 2015 as DOI: 10.1124/dmd.115.066076
This article has not been copyedited and formatted. The final version may differ from this version.

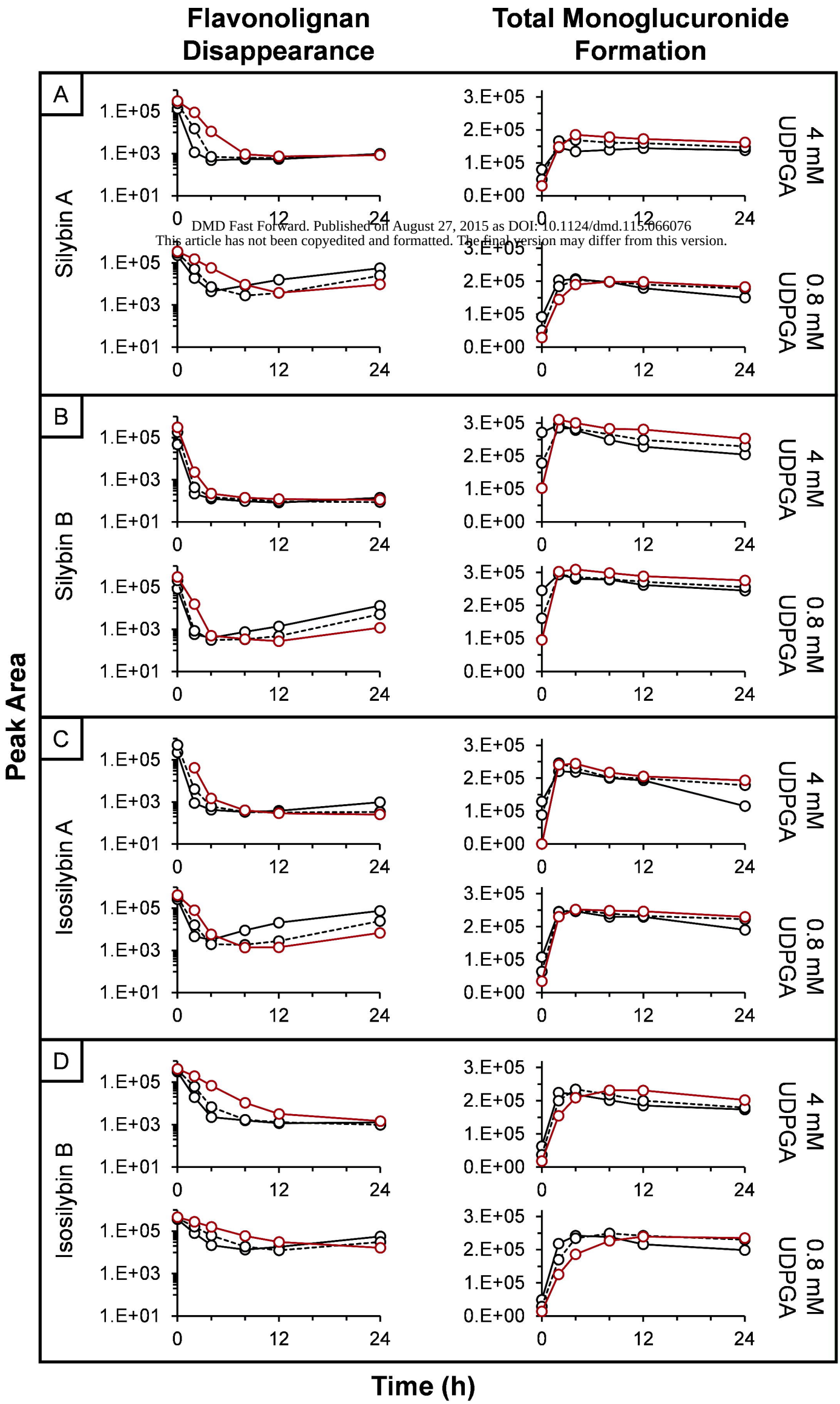

Figure 2

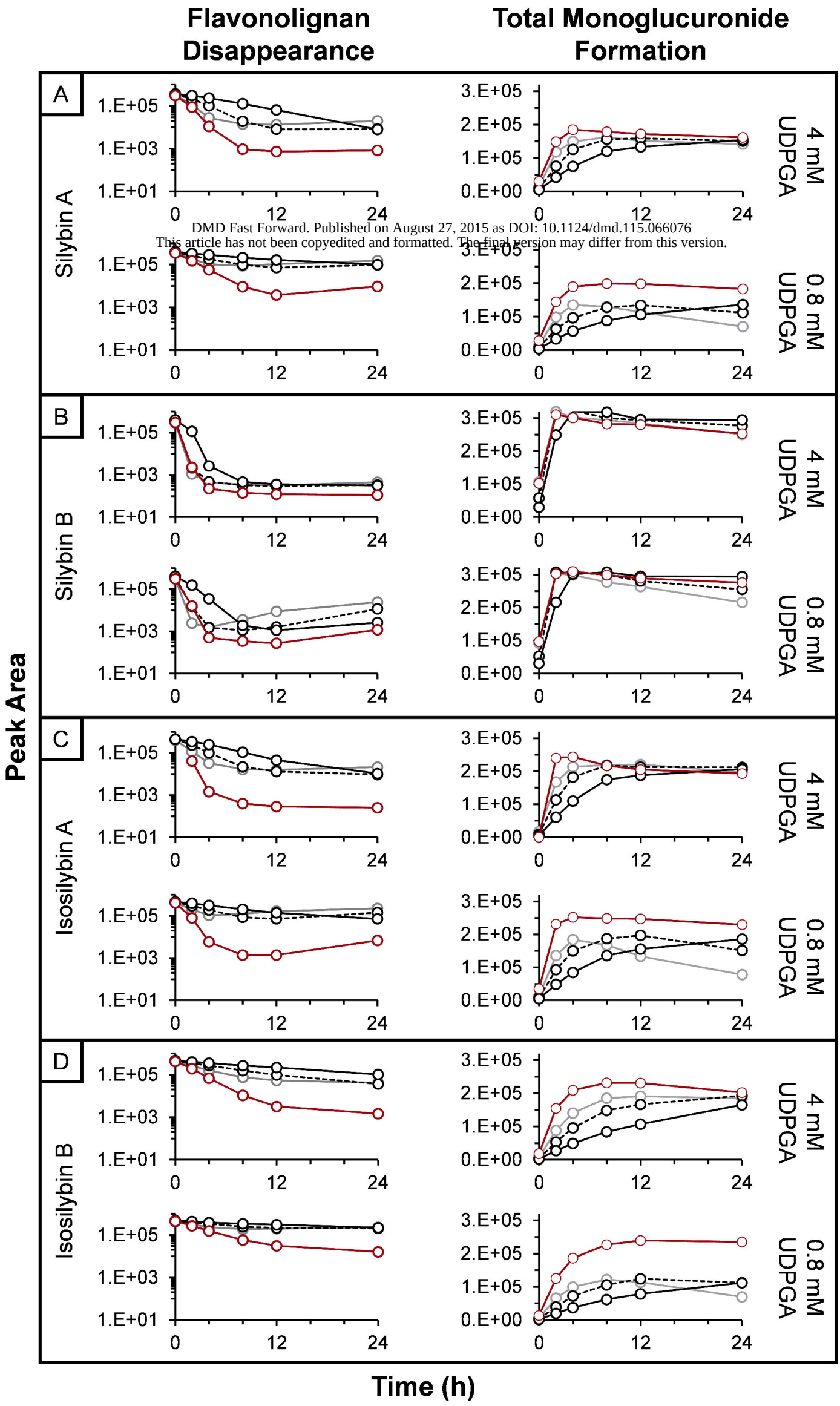

Figure 3

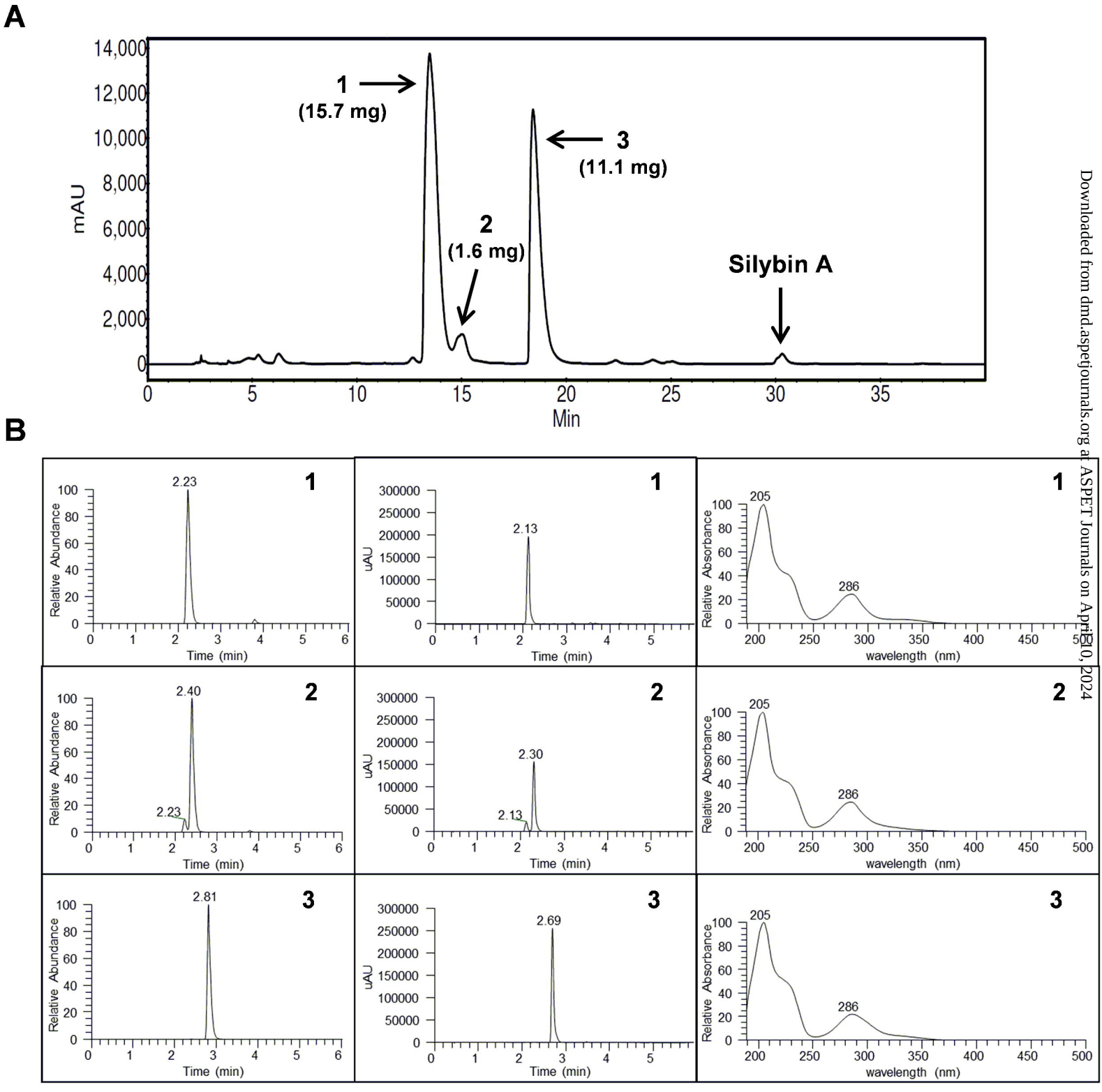

Figure 4

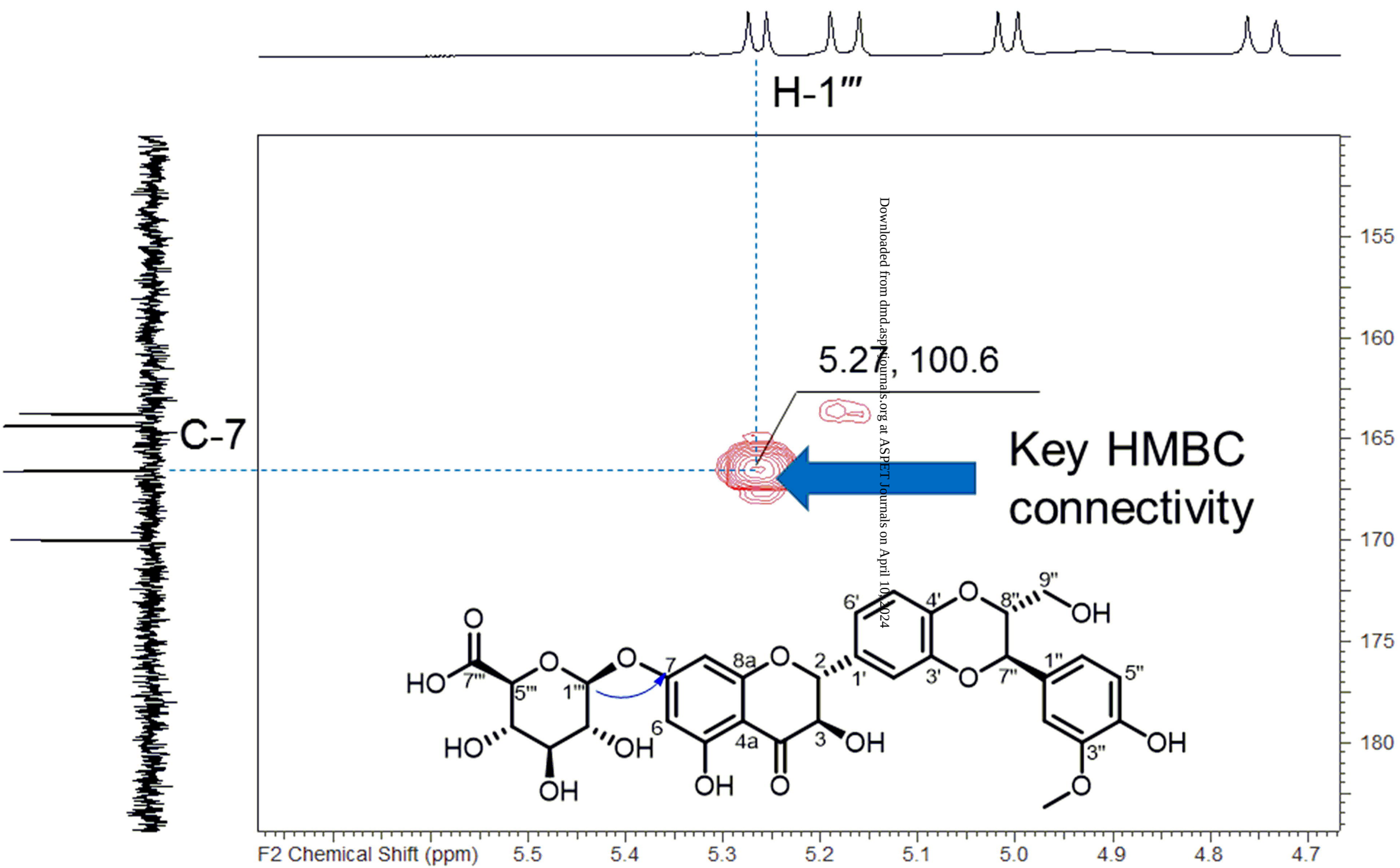

Figure 5

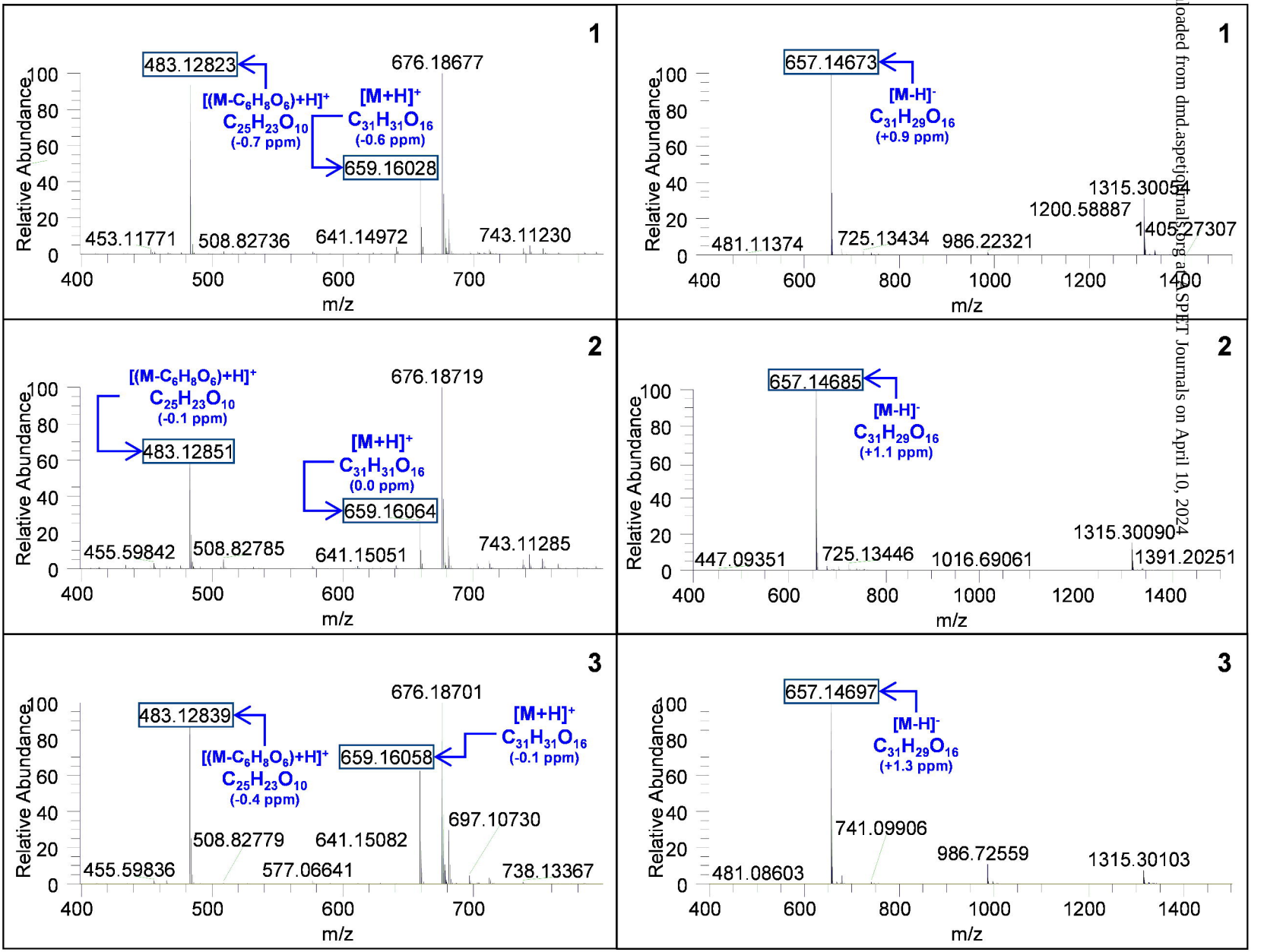

Figure 6

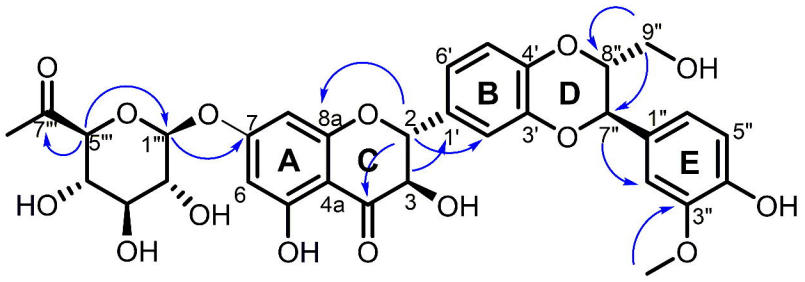

Silybin A-7-*O*-β-D-glucuronide (**1**)

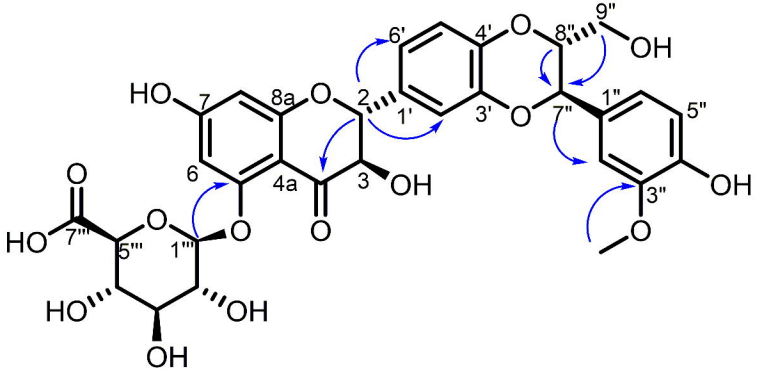

Silybin A-5-*O*-β-D-glucuronide (**2**)

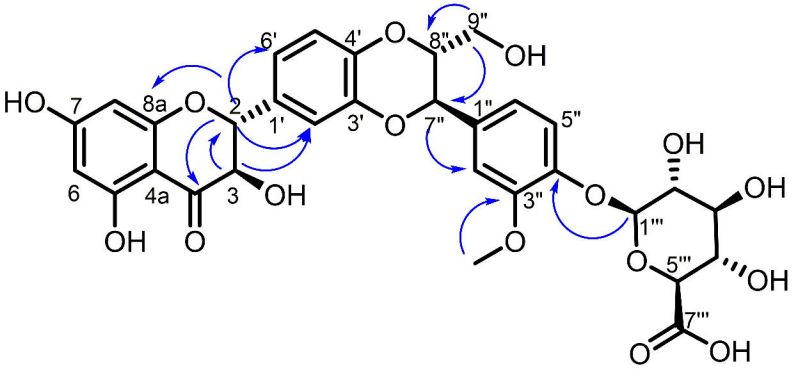

Silybin A-4´´-*O*-β-D-glucuronide (**3**)

Figure 7

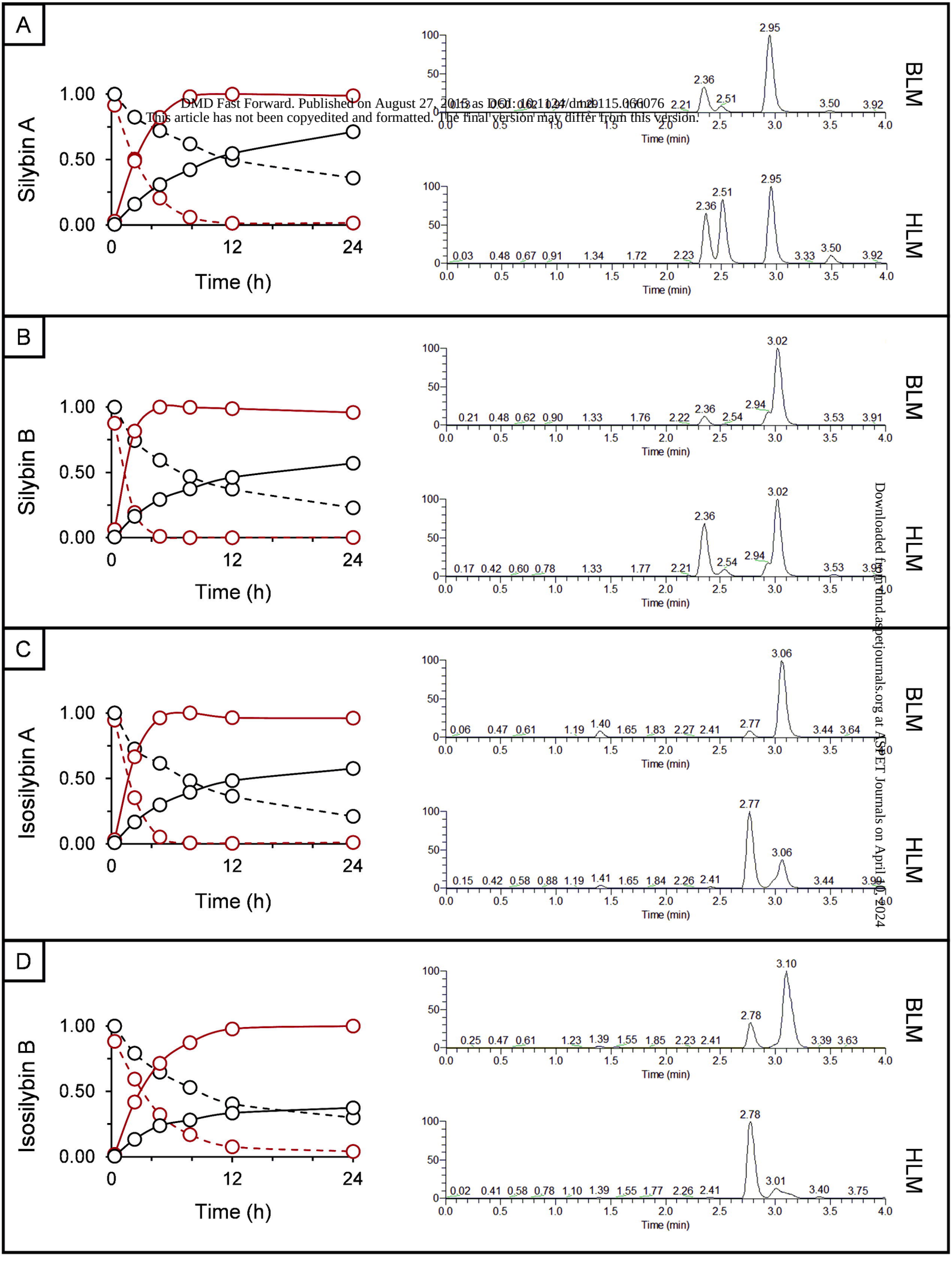

Figure 8

SUPPLEMENTAL DATA

Chemoenzymatic Synthesis, Characterization, and Scale-up of Milk Thistle Flavonolignan Glucuronides

Brandon T. Gufford, Tyler N. Graf, Noemi D. Paguigan, Nicholas H. Oberlies, and Mary F. Paine

Experimental and Systems Pharmacology (B.T.G, M.F.P), College of Pharmacy, Washington State University, Spokane, Washington; and Department of Chemistry and Biochemistry, The University of North Carolina at Greensboro, Greensboro, North Carolina (T.N.G, N.D.P., N.H.O)

Drug Metabolism and Disposition

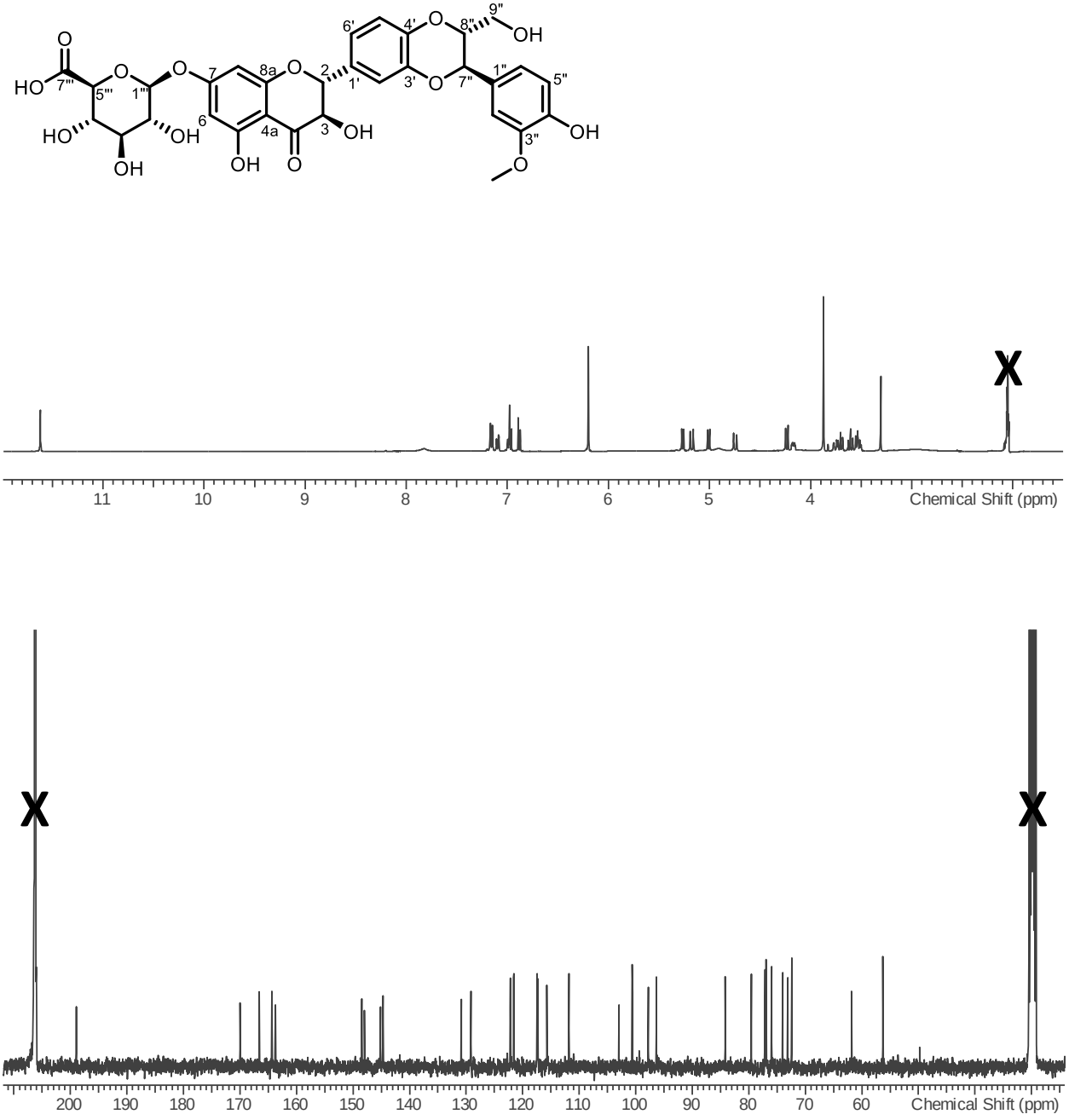

Figure S1. ^{1}H NMR (400 MHz; upper) and ^{13}C NMR (100 MHz; lower) spectra of **1** in acetone-d_6.

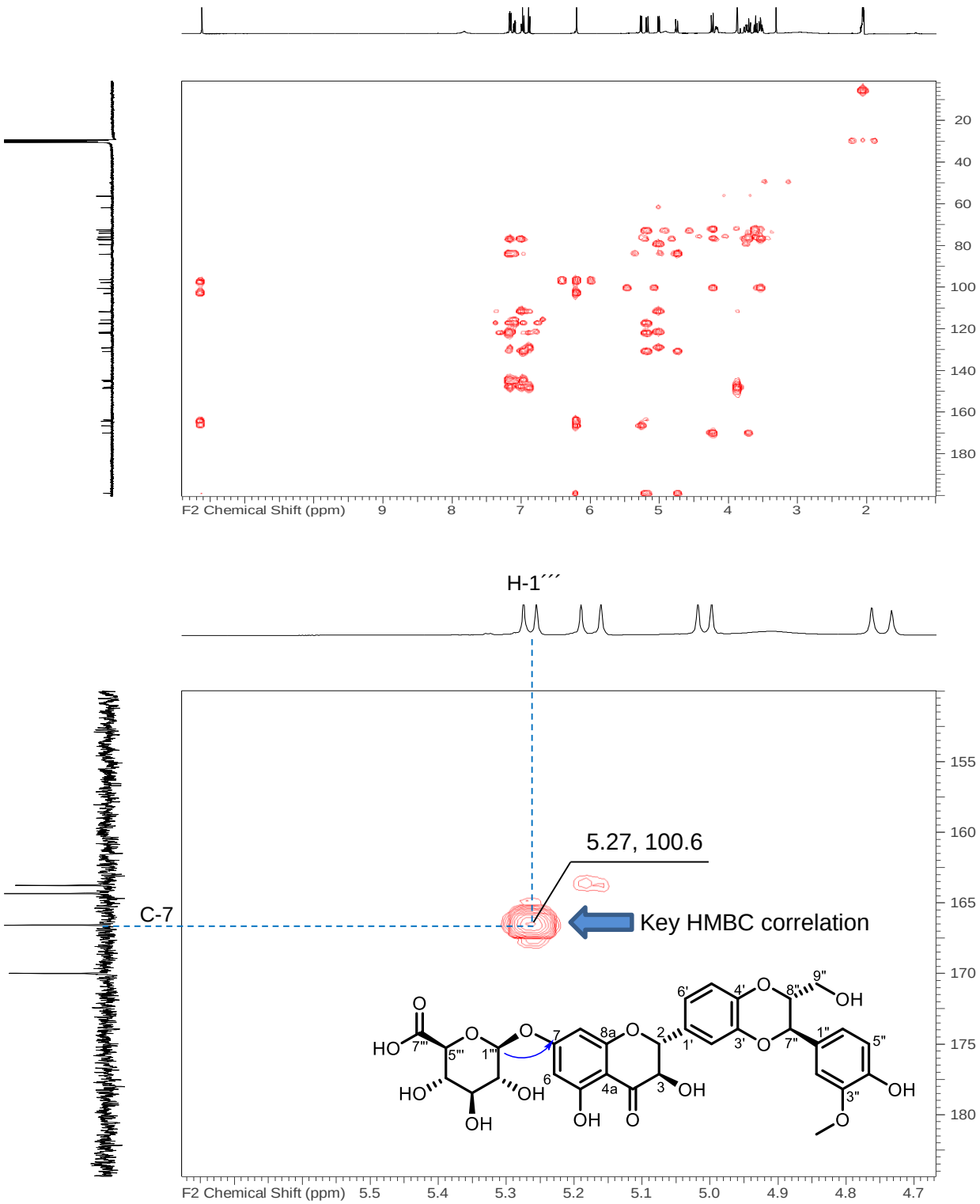

Figure S2. The HMBC spectrum of **1** (400 MHz/100 MHz) in acetone-d_6 (upper). The HMBC correlation from H-1´´´ to C-7 supported the assigned site of attachment of the glucuronide portion to the silybin A core, as illustrated (lower).

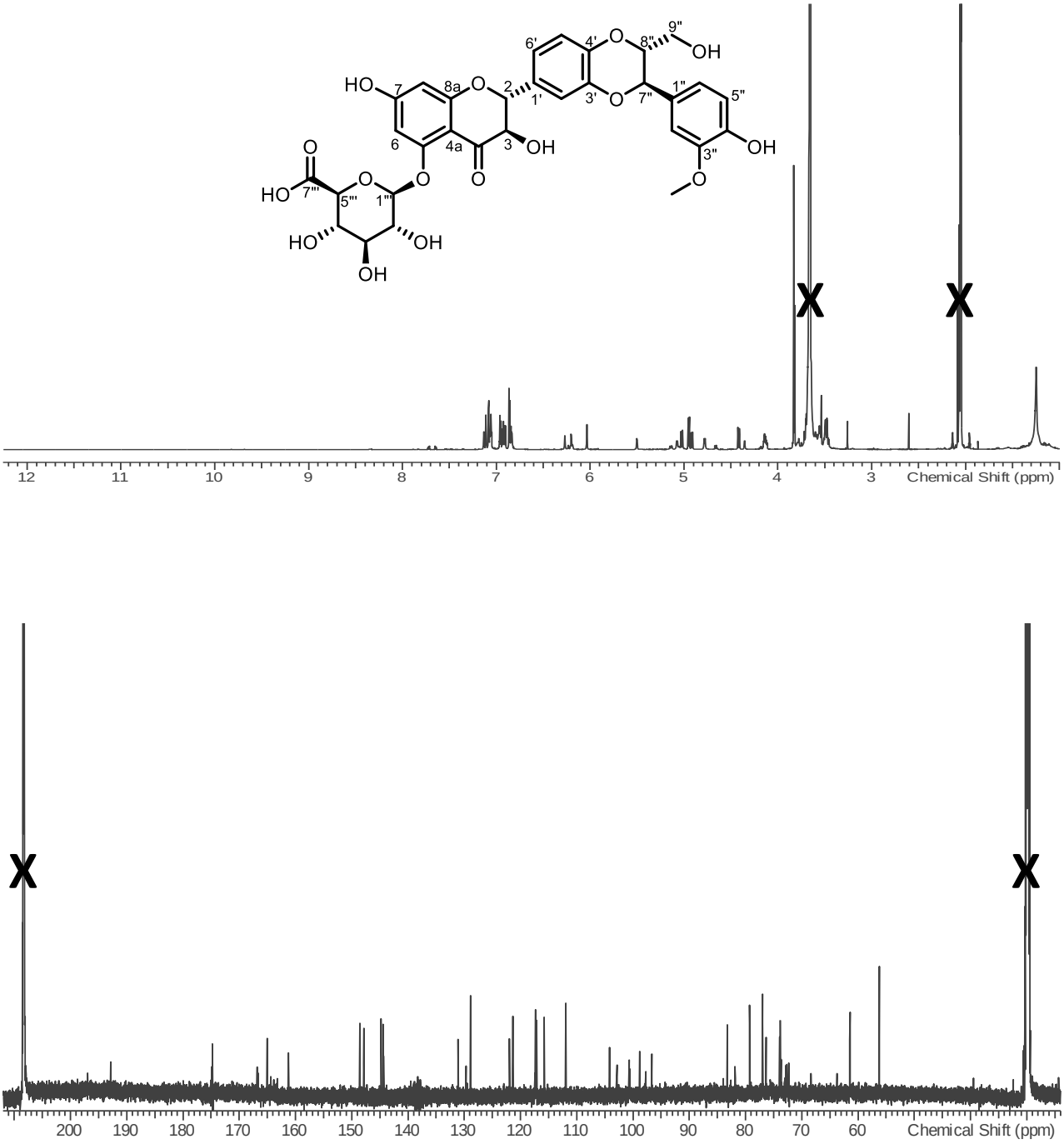

Figure S3. ^{1}H NMR (700 MHz; upper) and ^{13}C NMR (175 MHz; lower) spectra of **2** in 10% D_2O in acetone-d_6.

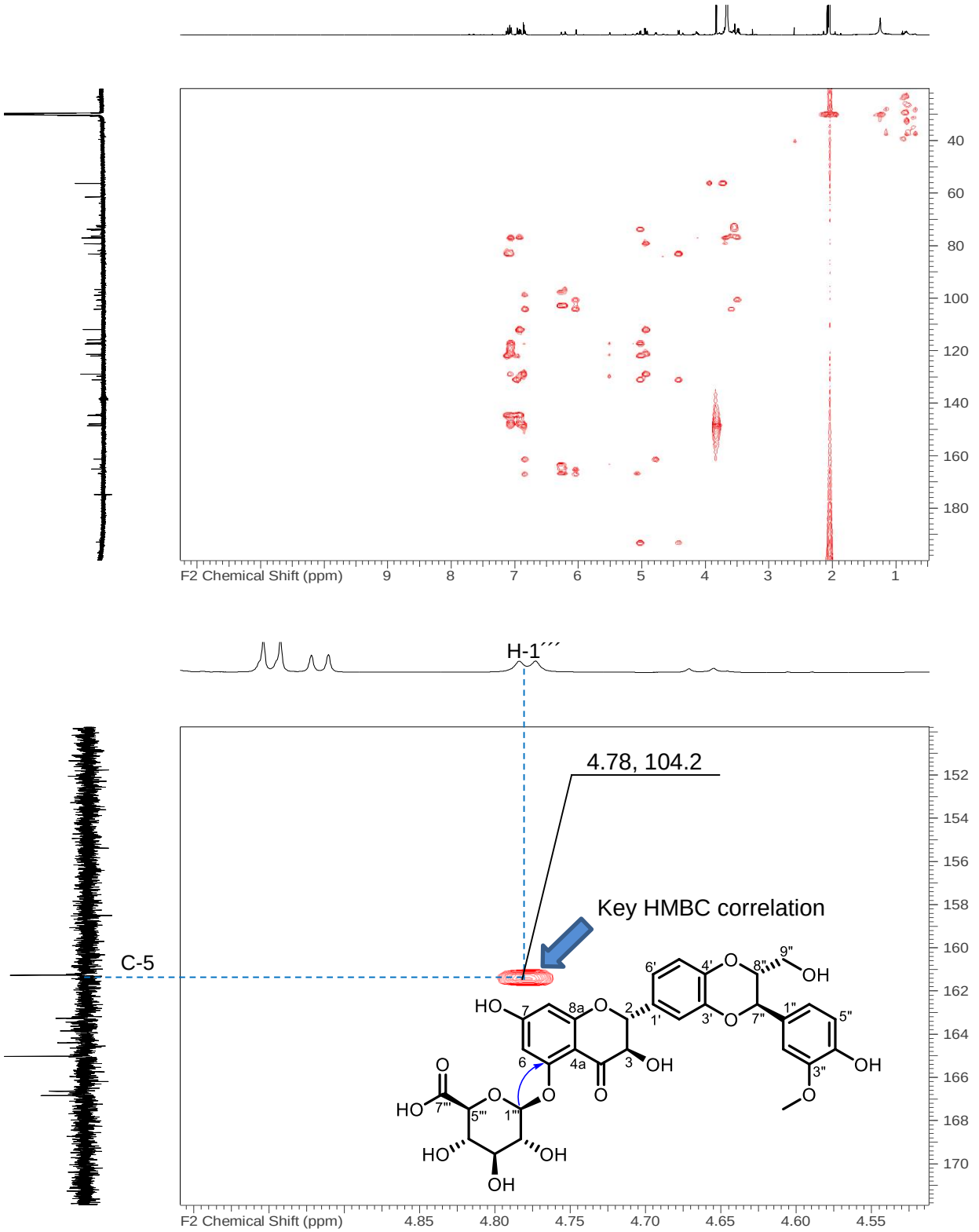

Figure S4. The HMBC spectrum of **2** (700 MHz/175 MHz) in 10% D_2O acetone-d_6 (upper). The HMBC correlation from H-1´´´ to C-5 supported the assigned site of attachment of the glucuronide portion to the silybin A core, as illustrated (lower).

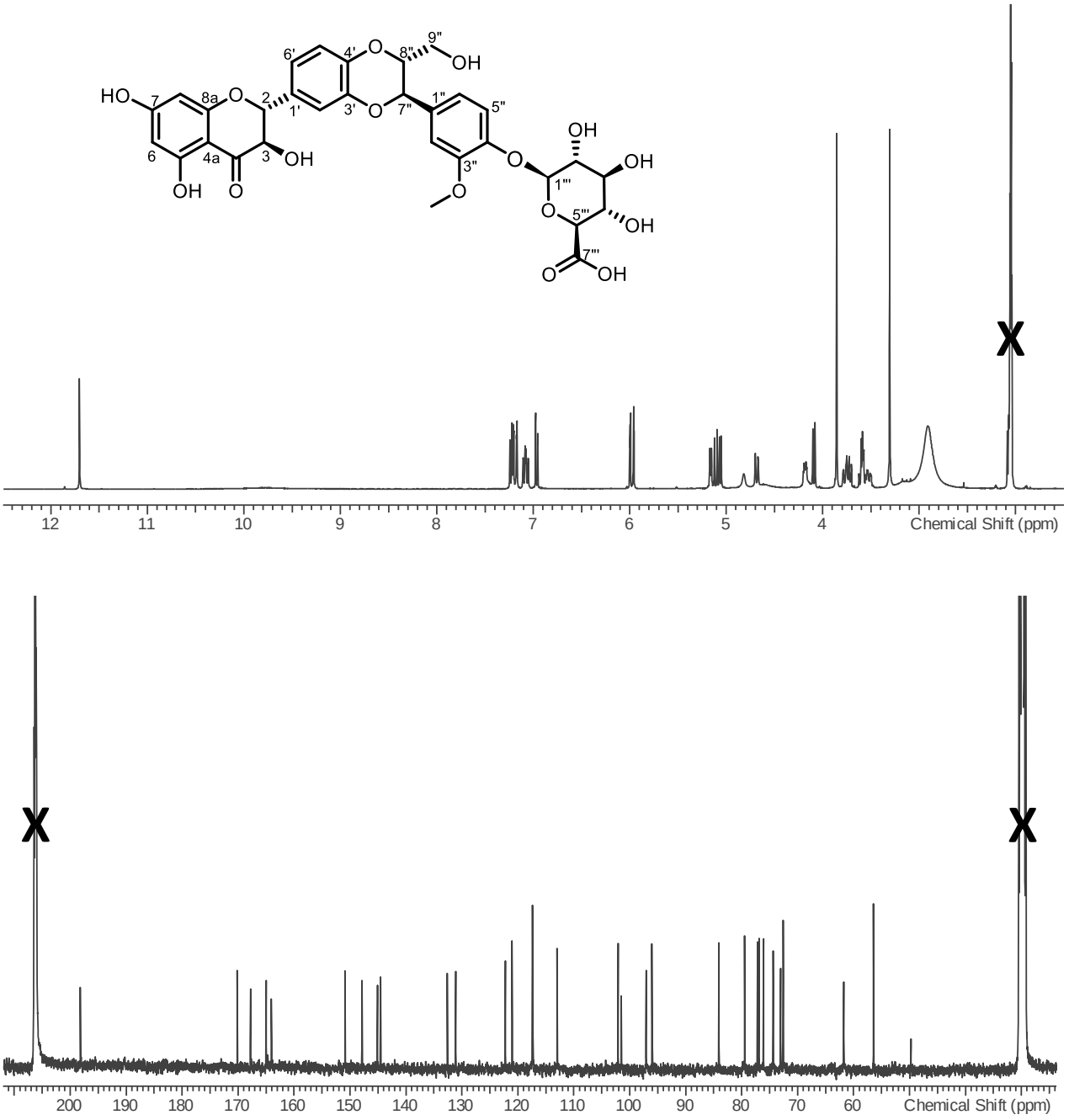

Figure S5. ^{1}H NMR (400 MHz; upper) and ^{13}C NMR (100 MHz; lower) spectra of **3** in acetone-d_6.

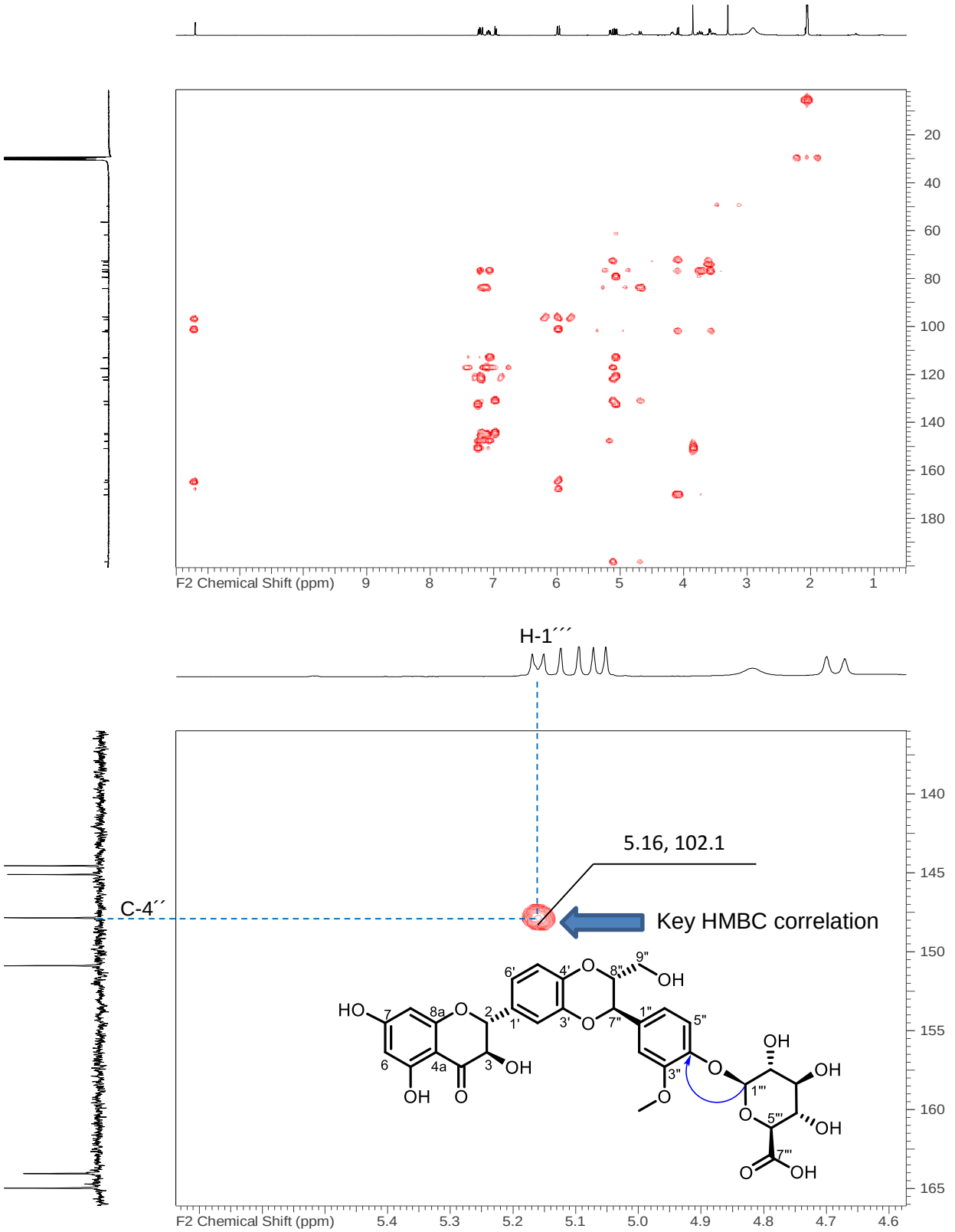

Figure S6. The HMBC spectrum of **3** (400 MHz/100 MHz) in acetone-d_6 (upper). The HMBC correlation from H-1´´´ to C-4´´ supported the assigned site of attachment of the glucuronide portion to the silybin A core, as illustrated (lower).